

**For Reference**

**NOT TO BE TAKEN FROM THIS ROOM**

Ex LIBRIS  
UNIVERSITATIS  
ALBERTAENSIS











THE UNIVERSITY OF ALBERTA

RELEASE FORM

NAME OF AUTHOR            T.E. MILNER  
TITLE OF THESIS            AN ELECTROPHYSIOLOGICAL STUDY OF THE  
                                 EFFECTS OF AXOTOMY ON SENSORY AND MOTOR  
                                 NERVE FIBERS  
DEGREE FOR WHICH THESIS WAS PRESENTED    MASTER OF SCIENCE  
YEAR THIS DEGREE GRANTED            FALL 1980

Permission is hereby granted to THE UNIVERSITY OF ALBERTA LIBRARY to reproduce single copies of this thesis and to lend or sell such copies for private, scholarly or scientific research purposes only.

The author reserves other publication rights, and neither the thesis nor extensive extracts from it may be printed or otherwise reproduced without the author's written permission.







THE UNIVERSITY OF ALBERTA

AN ELECTROPHYSIOLOGICAL STUDY OF THE EFFECTS OF AXOTOMY ON  
SENSORY AND MOTOR NERVE FIBERS

by

© T.E. MILNER

A THESIS

SUBMITTED TO THE FACULTY OF GRADUATE STUDIES AND RESEARCH  
IN PARTIAL FULFILMENT OF THE REQUIREMENTS FOR THE DEGREE  
OF MASTER OF SCIENCE

PHYSIOLOGY

EDMONTON, ALBERTA

FALL 1980



THE UNIVERSITY OF ALBERTA  
FACULTY OF GRADUATE STUDIES AND RESEARCH

The undersigned certify that they have read, and recommend to the Faculty of Graduate Studies and Research, for acceptance, a thesis entitled AN ELECTROPHYSIOLOGICAL STUDY OF THE EFFECTS OF AXOTOMY ON SENSORY AND MOTOR NERVE FIBERS submitted by T.E. MILNER in partial fulfilment of the requirements for the degree of MASTER OF SCIENCE.



## ABSTRACT

Medial gastrocnemius and sural nerves in one hindlimb of the cat were transected and prevented from regenerating. After periods ranging from 29-273 days compound action potentials were recorded in acute experiments from axotomized and contralateral control nerves upon stimulating the appropriate dorsal or ventral roots, or the nerves themselves.

Action potentials from single units were also recorded in a number of the same experiments. Amplitude was found to vary with the conduction velocity raised to powers ranging from about 1.5 to 2.3 and electrical charge with powers ranging from 1 to 1.8, while the duration varied inversely as approximately the square root of the conduction velocity.

Whole nerve conduction velocity distributions were computed on the basis of the relative number of single unit potentials of various conduction latencies required to generate the recorded compound action potential. A compound potential, obtained by stimulating the nerve in close proximity to the recording site, was used as a template for single unit potentials. The empirically observed relationships between amplitude, duration and conduction velocity were taken into account during the computation.

Conduction velocity distributions were analyzed to compare the rates of velocity decline of fast conducting (large) and slow conducting (small) sensory and motor fibers following axotomy. The conduction velocity of fast sensory



and motor fibers was found to decrease at different rates--sensory fibers slowing at a faster rate than motor fibers. Slow sensory and motor fibers showed little difference in the rate at which conduction velocity was reduced, slowing at approximately the same rate as fast motor fibers. Slow sensory fibers did, however, have a slower rate of decline than fast sensory fibers.

The conduction velocity distributions were also converted to electrical charges which were compared with the recorded charge values of the compound potentials in order to investigate the possibility of axon death. Although there was a significant loss of conducting axons following axotomy, it probably did not exceed 20-30% of the original number.

It is suggested that the difference in the effects of axotomy on axons of various functional groups may be related in part to the level of electrical activity they maintain, relative to their activity prior to injury.





## ACKNOWLEDGMENTS

I am deeply grateful to Dr. Richard Stein, who did the lion's share of the work in the acute preparations and who labored until the early hours of the morning, painstakingly dissecting filaments from spinal roots; but more than that, I am most thankful for his willingness to spend time discussing results and pointing me in the right direction in my attempts to sensibly interpret them.

I especially want to thank Brendon Hanley, who helped me with the initial surgery and shared the frustration of having to do it all again as we discovered the tenacity with which nerves regenerate.

Jean Gillespie must be commended for her perseverance, doing her best to provide us with a description of the morphology of our degenerate axons, despite the poor samples which she often had to work with. Thanks again to Jean and Brendon for patiently enduring the tedium of counting fibers.

I wish to thank Tessa Gordon for assisting in the dissection and for encouraging me to learn some history.

Without Robert Rolf this work would have proceeded with much less efficiency. I appreciate his technical assistance immensely, but it is as a personal friend that I value him the most. He always took time to examine my problems and when he did not have the answers he often provided necessary insight.



## Table of Contents

Chapter	Page
I. INTRODUCTION .....	1
II. METHODS .....	8
III. RESULTS .....	16
IV. DISCUSSION .....	49
V. SUMMARY .....	57
REFERENCES .....	58
APPENDIX I .....	62
APPENDIX II .....	66



## List of Tables

Table	Description	Page
I	Regression analysis of single unit potential dependence on conduction velocity.....	23
II	Regression analysis of conduction velocity decay curves.....	32
III	Regression analysis of compound action potential charge decay curves.....	40





## List of Figures

Figure	Description	Page
1	Electrode arrangement and typical sural compound action potentials.....	11
2	Single unit potential template and typical MG nerve single unit potentials.....	15
3	Conventional and cumulative sural conduction velocity distributions.....	17
4	Histological and electrophysiological sural conduction velocity distributions.....	20
5	Sural single unit potential data.....	24
6	MG sensory single unit potential data.....	25
7	MG motor single unit potential data.....	26
8	Progressive changes in the conduction velocity distribution of axotomized sural nerves.....	28
9	Conduction velocity decay curves .....	33
10	Progressive changes in sensory conduction velocity distributions of axotomized MG nerves...	35
11	Progressive changes in motor conduction velocity distributions of axotomized MG nerves...	37
12	Decay curves for spinal root compound action potential charge.....	41
13	Exponential decay curves for nerve compound action potential and computed charge.....	43
14	Asymptotic decay curves for nerve compound action potential and computed charge.....	48



## I. INTRODUCTION

Severing a mammalian peripheral nerve initiates a reaction proximal to the point of lesion which leads to morphological and electrophysiological changes in individual axons. Both axon diameter and total diameter (axon + myelin) are reduced (Fleming, 1896) and conduction velocity slows as the fiber diameter decreases (Kiraly & Krnjević, 1959, Cragg & Thomas, 1961). Axons die back from the severed end and then attempt to re-establish functional connections by sending out sprouts from the terminals (Young, 1942), though reversal of the proximal degeneration occurs only if there is reinnervation (Gutmann & Sanders, 1943). Restoration of function promotes recovery of axon diameter and conduction velocity (Cragg & Thomas, 1964).

Prevention of functional recovery does not necessarily lead to complete loss of axonal function. Spontaneous and evoked neural activity can be recorded long after a nerve has been severed (Govrin-Lippmann & Devor, 1978, Davis et al., 1978, Stein et al., 1979). Although the magnitude of the activity declines for some months following section of the nerve, it may eventually approach a steady-state level (Stein et al., 1979).

Whether all axons in a severed nerve degenerate to the same extent or whether there are differential effects corresponding to the functions originally subserved is a question which has not been conclusively answered. Early histological observations suggested that axons in the dorsal



roots deteriorated more than axons in the ventral roots following amputation (Fleming, 1896) or nerve section (Bucy, 1928). Later it was demonstrated that conduction failed sooner in the degenerating distal segment of a severed sensory nerve than in a muscle nerve (Gutmann & Holubář, 1949). Responsiveness (a measure of the absolute refractory period) of muscle nerves was little different in the ventral root but declined markedly in the dorsal root following nerve section (Király & Krnjević, 1959). Chronic recordings from cat peripheral nerves also indicated that the degenerative process might be more severe for sensory than for motor axons (Stein et al., 1979). A more systematic study was then undertaken to quantify these differences (Hoffer et al., 1979).

Compound action potentials were recorded from dorsal and ventral roots following stimulation of normal and previously severed sensory and muscle nerves. The electrical charge measured from dorsal root compound action potentials was found to deteriorate more rapidly than that of ventral root compound action potentials over a period of approximately 250 days. Although distinguishing between sensory and motor axons, this type of analysis did not provide the detail necessary to resolve possible differential effects on axons classified according to size or conduction velocity.

It is well-known that the function subserved by an axon is related to its conduction velocity (Erlanger, 1927).





Consequently, there has been considerable interest, particularly among clinicians, in developing a means to compute conduction velocity distributions for whole nerves. Several mathematical approaches have been described but the basic principle is similar in all cases.

The compound action potential is assumed to be the linear sum of single unit action potentials which arrive at the recording site at latencies dependent on the distance from the site of stimulation and the axonal conduction velocity. By constructing a model single unit potential and accounting for its dependence on conduction velocity it is then possible to compute a conduction velocity distribution from the compound action potential.

Gasser and Erlanger (1927) first suggested the idea by reconstructing a compound action potential from the fiber diameter histogram of a nerve. The histogram was converted to a normalized distribution of triangular potentials of varying latency. This involved transformation of fiber diameter to conduction velocity together with scaling of potential amplitude according to the number and diameter of fibers represented. The potentials were then summed point by point to produce the compound action potential. Buchthal and Rosenfalck (1966) pursued this approach further in the clinical analysis of compound action potentials recorded from human sensory nerves.

Landau et al. (1968) simplified the original procedure by introducing a single scaling factor relating the compound





action potential amplitude to the number and diameter of fibers, thus converting individual bins of the fiber diameter histogram directly to points on the compound action potential.

With the advent of computers it was no longer necessary to make as many simplifications. Olson (1973) worked with a detailed mathematical model of the compound action potential based on the summation of single unit potentials, which could vary not only in latency and amplitude, but also in shape and duration. His computer-based model allowed reconstruction of a compound action potential from the normalized nerve fiber diameter histogram. He made a detailed study of the model's sensitivity to axon geometry and fiber distribution within the nerve trunk and to the relationship between fiber diameter, conduction velocity and single unit potential amplitude, including as well, the effects of the duration and rise time of the single unit potential. Once the model had been optimized it could be used to predict the nerve fiber diameter histogram or the conduction velocity distribution corresponding to a particular compound action potential.

Because the electromyogram is easier to record clinically than the neurogram, attempts have been made to determine alpha-motoneuron conduction velocity distributions from compound muscle action potentials. Lee et al. (1975) used the waveform of averaged single motor units to reconstruct the muscle compound action potential. The number



and distribution of conduction velocities of the motoneurons was varied in order that the summation of their action potentials resulted in a compound action potential most closely approximating the recorded muscle compound action potential.

An alternative method (Leifer et al., 1977) used a sequence of stimuli at two points along the muscle nerve to selectively occlude the responses of groups of motor units by varying the interval between the proximal and distal stimuli. Motor units with conduction latencies greater than the interstimulus interval were not activated due to occlusion of orthodromic and antidromic impulses along the nerve fiber. The recorded muscle compound action potential was quantified by cross-correlating the response to proximal stimulation only, with that actually recorded for a particular interstimulus interval. The normalized cross-correlation function was then plotted cumulatively against the interstimulus interval. After differentiating and correcting for the effects of relative refractory period, the normalized latency distribution was obtained. This could then be easily converted to a conduction velocity distribution.

Recently, Barker et al. (1977) presented a method for computing the conduction velocity distribution using a model very similar to that of Olson. By assuming that any single unit potential could be represented by a model single unit potential scaled according to its conduction velocity the



compound action potential could be simply represented as the linear sum of single unit potentials. Sampling the compound action potential at  $M$  discrete intervals produced a set of  $M$  linear simultaneous equations which could be solved to determine the conduction velocity distribution. The model single unit potential was obtained by stimulating near the recording site on the nerve. This minimized the effects of dispersion due to differences in the conduction velocities of stimulated fibers hence providing a model which represented the average shape of a single unit potential.

Cummins et al. (1979) generalized this approach to allow modification of parameters as suggested earlier by Olson. This formulation was chosen for analysis of compound action potentials recorded in the experiments of the present study. The mathematical theory and computer implementation are described in greater detail in Appendix I. Kovacs et al. (1979) developed a similar method which differed only in the means used to solve the system of equations.

An alternative solution suggested first by Williams (1972) for the purpose of studying the information-processing characteristics of nerves, was adapted to the problem of computing the nerve conduction velocity distribution and tried initially. The compound action potential was viewed as the output of a discrete-time linear system characterized by an impulse response whose input was the single unit potential waveform. Appropriate scaling of the impulse response with respect to latency







produced a latency distribution which could be converted to a conduction velocity distribution. The impulse response could be obtained in several ways, one of the simplest being to use the Fast Fourier Transform. Several sources of error reduced the reliability of the results obtained in this way; therefore, it was felt that Cummins' solution was more satisfactory. Cummins also tried the linear systems approach but abandoned it for similar reasons (personal communication).

By computing conduction velocity distributions from compound action potentials recorded from normal and severed nerves, differential effects of axotomy on various classes of fibers become apparent. The point of this study was to use the conduction velocity distribution to infer the viability of severed axons which had been categorized according to conduction velocity classes.



## II. METHODS

Data were obtained from experiments conducted on 26 adult cats of both sexes, 9 of which were normal animals and 17 in which the sural and medial gastrocnemius (MG) nerves of the left hindlimb had been surgically sectioned some time prior to the experiment. Transection of the nerves was performed under aseptic conditions. The animals were initially anesthetized with Nembutal and maintained on Halothane for the duration of surgery. The nerves were ligated proximal and distal to the point of section and then cut cleanly with scissors. The MG nerve was severed near its point of entry into the MG muscle and the sural nerve distal to the midpoint of its course over the lateral gastrocnemius muscle. The proximal stump of the severed nerve was sutured to a Silastic sheet approximately 1 cm square. Care was taken to prevent reinnervation by reflecting the MG nerve away from its muscle and suturing the Silastic sheet to more proximal muscles. In the case of the sural the sheet was turned over onto the nerve and sutured to the lateral gastrocnemius muscle. In some of the earliest attempts the precautionary procedure was not as thorough and reinnervation did occur.

Acute experiments under deep Nembutal anesthesia were conducted after periods ranging from 29-273 days following initial surgery. Nerves and spinal roots of both hindlimbs were prepared for stimulation and recording. The right hindlimb served as a control. Spinal roots from the L6 to S2



levels were exposed bilaterally by laminectomy. Extensive denervation of the hindlimbs was required to minimize artifact due to muscle activity when stimulating ventral roots. All branches of the sciatic nerve with the exception of the two nerves of interest were cut. The MG and sural nerves were then dissected free from surrounding tissue over a length of 15-25 mm. These nerves were otherwise left intact until the time of recording.

When dissection was complete the cat was mounted in a stereotaxic frame with both hindlimbs in extension and securely clamped at the knee and ankle. Except for one experiment, the control nerves were prepared for recording first. Paraffin oil pools fashioned from skin flaps bathed the spinal cord and the hindlimb nerves. Their temperature was maintained at  $36^{\circ} \pm 2^{\circ}\text{C}$  by radiant heat. Body temperature was kept in the same range by means of a thermostatically controlled heating pad.

The spinal roots were separated and cut near their point of entry into the cord. L7 and S1 dorsal or ventral roots were placed on a 6 hook electrode array (2.5 mm interelectrode spacing) which served for both stimulating and recording purposes. The first nerve (the MG in most experiments) was ligated and cut distal to the ligature just before recording. Axotomized MG nerves were cut 5-10 mm proximal to the neuroma; sural nerves, being somewhat longer, were cut more than 20 mm from the neuroma. A bipolar stimulating electrode consisting of two hooks was placed in





contact with the nerve at a point 3-8 mm proximal to the first hook of the recording array. The nerve was placed on a 6 hook array (3 mm interelectrode spacing) in such a way that the ligature just passed over the most distal hook. Monopolar potentials were recorded with respect to the cut end after crushing the nerve between the two most distal hooks. The configuration is represented schematically in Figure 1A.

Before recording compound action potentials the impedance was measured at each hook with respect to the most distal hook with an impedance meter using a 10 kHz test signal. At 10 kHz the capacitive component of the impedance was small (phase angle less than  $10^0$ ) making the impedance almost purely resistive. By plotting the impedance values against the relative position of each hook, the net tissue impedance (contact impedance of the nerve) could be determined from the point at which a line, fitted by eye, intercepted the impedance axis. Occasionally, a negative intercept was observed; the contact impedance was then set to zero. Subtracting the contact impedance from the impedance measured over the recording length gave the net recording impedance.

Nerves and roots were stimulated with negative rectangular pulses of 0.01 msec duration at rates not exceeding 20 Hz. Stimulation of the nerve at the point near the recording array produced a compound action potential with little dispersion resulting from differences in the





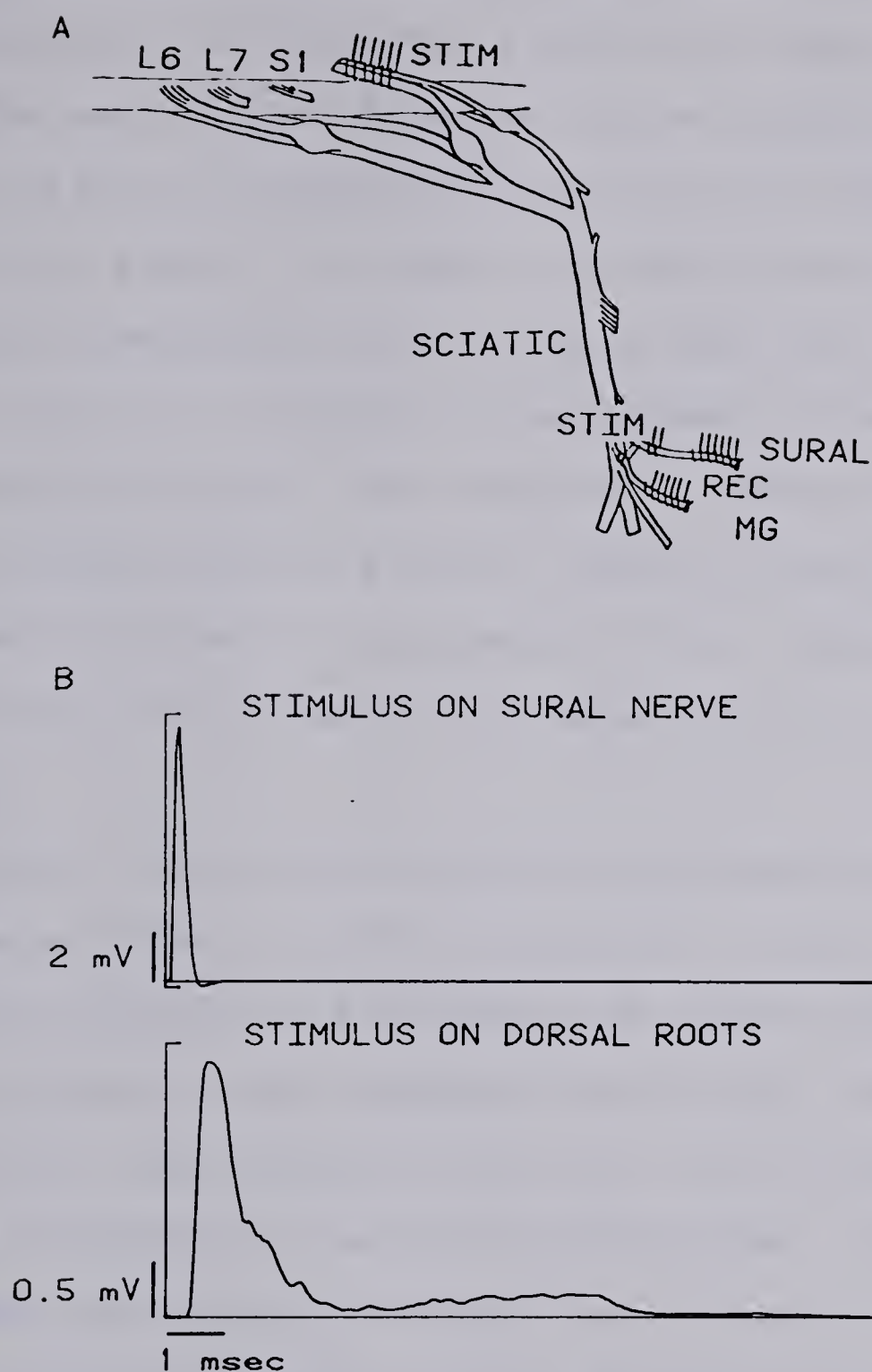


Figure 1

A. Schematic representation of nerves prepared for stimulating and recording showing approximate placement of electrode arrays. B. Comparison of sural nerve compound action potentials recorded while stimulating close to the recording site (upper trace) and at the dorsal roots (lower trace). The lower compound action potential has been delayed by 1.5 msec, slightly less than the latency of the fastest conducting sural fibers. Note that it is dispersed considerably as the result of relatively large differences in the latencies of fast and slow conducting fibers.



conduction velocities of activated fibers. Stimuli delivered to the nerve were adjusted so that a near maximal response was recorded from the fastest conducting fibers, with little or no detectable contribution from slower conducting fibers. In order to minimize the stimulus artifact produced by stimulating so near the recording site, a short stretch of the MG nerve between stimulating and recording points was left attached to the main trunk of the sciatic nerve while a similar length of the sural nerve remained attached to surrounding tissue. Generally, the first one or two hooks of the recording array were grounded as well.

Spinal roots were stimulated supramaximally for myelinated fibers (10-20X threshold) in order to record the compound response of all conducting fibers. The compound action potential was dispersed considerably due to the relatively long conduction distance which accentuated the effect of conduction velocity differences. Figure 1B compares the response recorded from the sural nerve when stimulating the nerve with that obtained from dorsal root stimulation. In a little over half the experiments the nerve was stimulated supramaximally and compound action potentials were recorded from the spinal roots as well.

Recorded potentials were displayed on a storage oscilloscope and on a computer generated CRT display while being digitized and averaged. Signals were sampled and digitized using a 10 bit A/D convertor. Control compound



action potentials were sampled at a rate of 20 kHz while compound potentials from axotomized nerves, because of their longer duration due to slower conducting fibers, were usually sampled at lower rates. Generally, the longer the time which had elapsed since axotomy the lower the sampling rate. The lowest rate ever used was 6 kHz. Single unit potentials were sampled at 50 kHz. Each potential was stored as a 256 point array. Averages normally consisted of 50 sweeps but occasionally up to 250 were accumulated, particularly when signal to noise ratio was low. Averaged potentials were then stored on disc for later processing and analysis. Data acquisition, processing and analysis was carried out using programs written for a PDP11/34 computer.

Once recording from the first nerve was complete the second nerve was prepared in the same manner and recording followed a similar sequence. The contralateral hindlimb was treated in the same way.

In 11 of the experiments dorsal and/or ventral root filaments were teased apart and individually stimulated in order to record single unit potentials from the nerves. The potentials were recorded and averaged like the compound action potentials.

Nerve samples were taken from the region of recording and fixed for histological examination. Experiments were normally terminated with an overdose of Nembutal. Nerves were then exposed over their entire course and conduction distances measured from lengths of thread laid along the





nerve.

Compound action potentials and single unit potentials were analyzed using a computer program which could determine the amplitude and half-width of a peak, as well as calculating the area under the peak. The recorded potential amplitude could be converted to dimensions of current by dividing the amplitude by the recording impedance measured at 10 kHz. Computation of the area was then equivalent to integrating current over time, giving dimensions of charge.

Another program was used to compute conduction velocity distributions. The compound action potential obtained by stimulating the nerve near to the recording site served as a single unit potential template. That it did indeed represent the average shape of a single unit potential was confirmed by comparing its shape with that of single unit potentials of different conduction velocities recorded later from the same nerve (Figure 2). The relative number of single unit potentials of various conduction velocities required to reconstruct the dispersed compound action potential obtained from spinal root stimulation, could then be computed. The computation incorporated scaling factors which accounted for the dependence of amplitude and duration of single unit potentials on conduction velocity. These factors were determined from the accumulated single unit potential data. A description of the computer program is included in Appendix I.



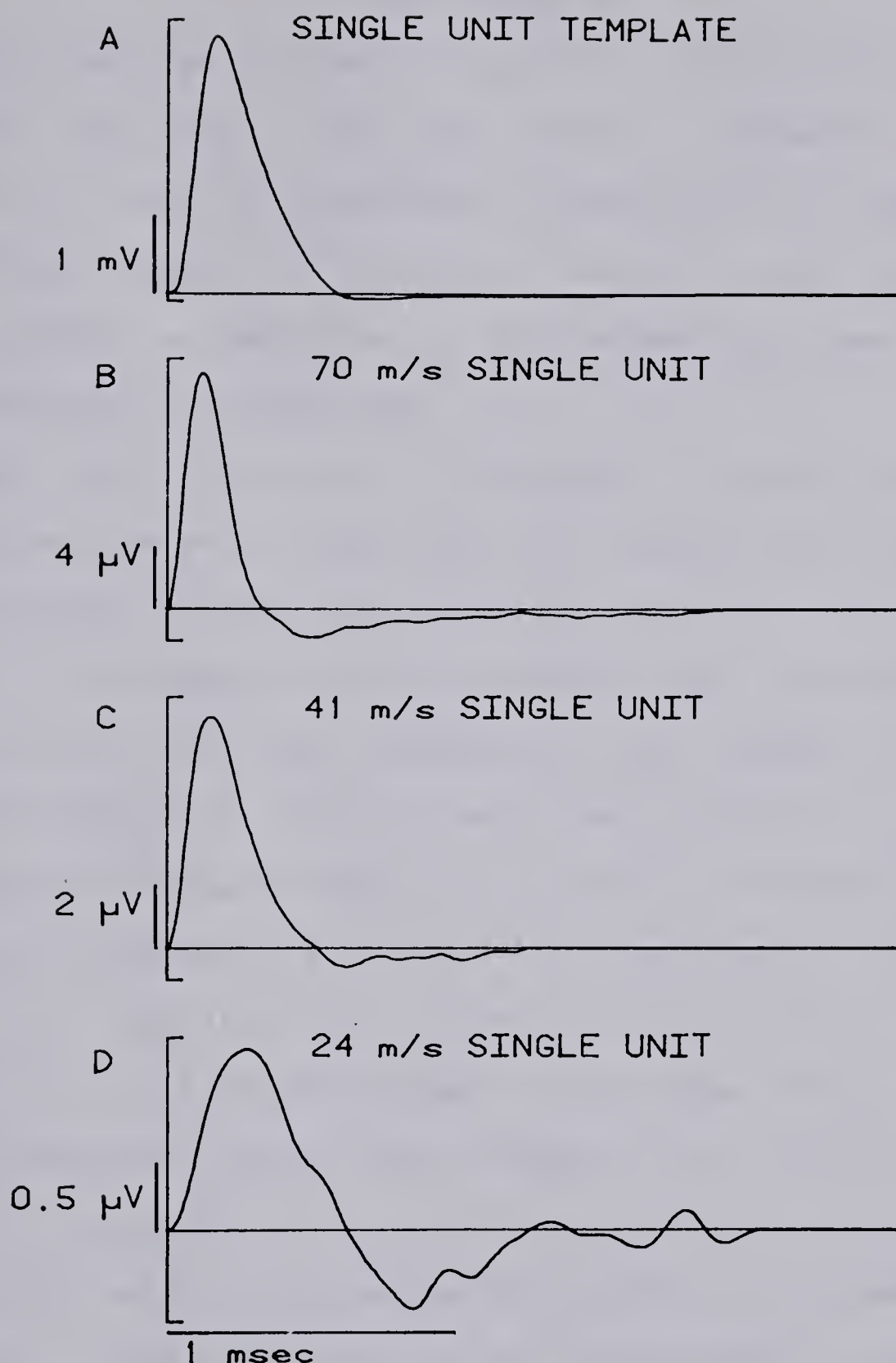


Figure 2

A. The compound action potential obtained by stimulating an MG nerve near the site of recording to provide a template of the average shape of a single unit potential. B, C and D. Single unit potentials of different conduction velocities recorded from the same nerve. Note that the positive phases of the waveforms are quite similar.



### III. RESULTS

Figure 3 compares the mean conduction velocity distributions obtained from control and contralateral axotomized sural nerves of 7 cats in experiments conducted 29-71 days following axotomy. The conduction velocity distributions were computed as described in the Methods and have been plotted here in three forms.

The first (Figure 3A) is plotted in conventional histogram form on a linear scale of conduction velocity with bins of equal width. The conduction distance, the latency to onset of the compound action potential and the sampling rate determine the bin width. Because of the inverse relationship between conduction velocity and time, conduction velocity increments corresponding to the sampling intervals of the digitized compound action potential decrease as the conduction time increases. Using histogram bins of equal width fails to take advantage of the higher resolution at lower conduction velocities offered by this relationship.

In Figure 3B the bin width is allowed to decrease as conduction velocity decreases providing a consequent increase in the resolution of the percentage of slow conducting fibers. This was accomplished by a threefold increase in the number of histogram bins. Note that the histograms have been plotted on a logarithmic scale of conduction velocity and hence the bin widths appear approximately equal. The choice of a logarithmic scale was prompted by the need for a simple method of qualitatively





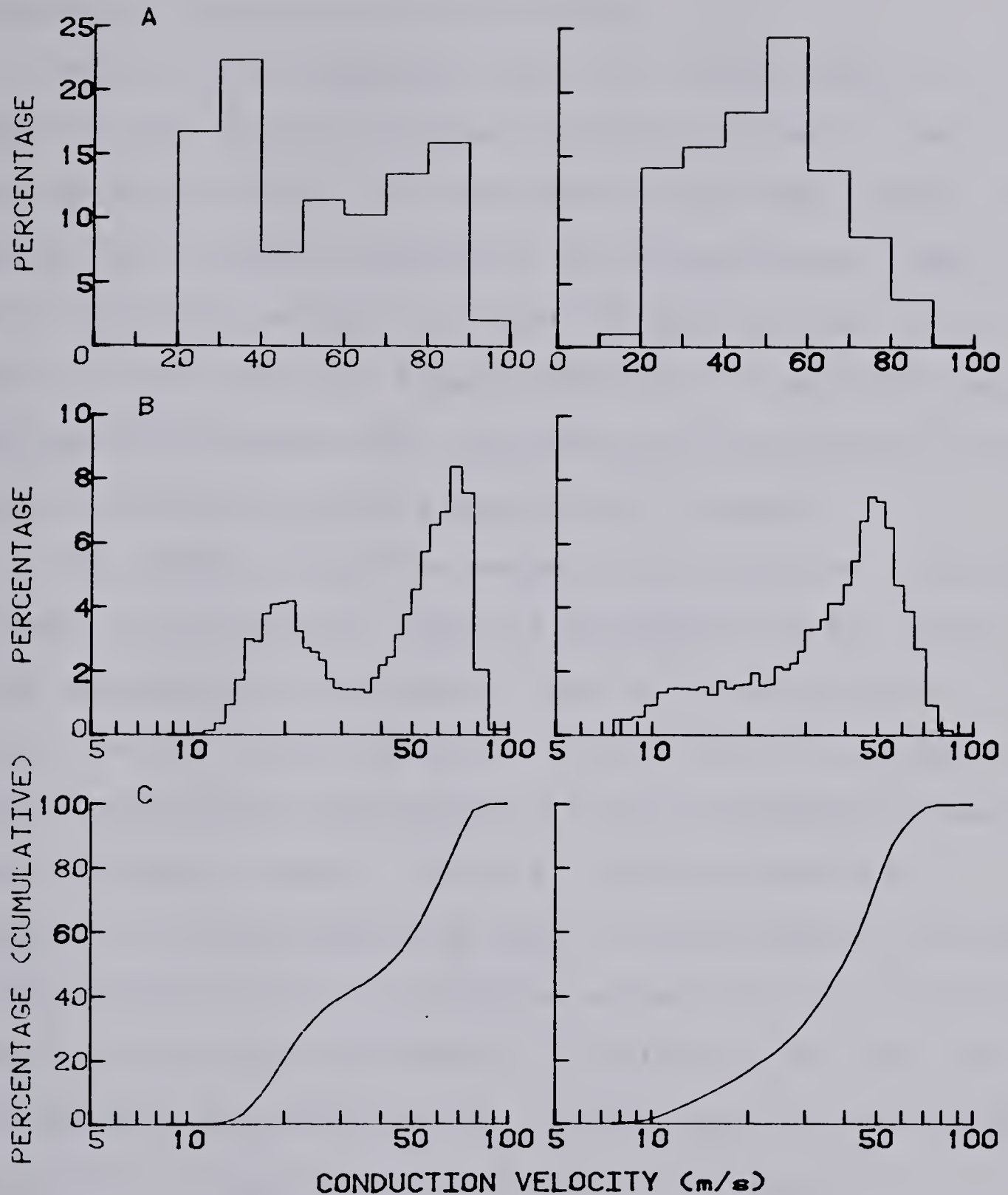


Figure 3

The mean conduction velocity distributions for control (left) and axotomized (right) sural nerves 29-71 days following axotomy plotted as: A. Conventional histograms on a linear scale of conduction velocity; B. Conventional histograms on a logarithmic scale of conduction velocity; C. Cumulative histograms on a logarithmic scale of conduction velocity. Refer to text for explanation.





comparing the relative effects of axotomy on fast and slow conducting fibers, as explained below.

Cumulative histograms (Figure 3C) proved useful in comparing the conduction velocity distributions of control and axotomized nerves. For any given conduction velocity the cumulative histogram represents the percentage of fibers in the distribution which conduct at velocities less than or equal to that velocity. Figures 3B and 3C illustrate how the features of a conventional histogram are manifested in the shape of the corresponding cumulative histogram.

The control conduction velocity distribution is bimodal in nature. As a result, there is a region with few fibers which separates the two peaks. This is reflected as a plateau in the rising curve of the cumulative histogram. The conduction velocity distribution of the axotomized nerves is nearly unimodal; hence, there is little evidence of a plateau in the corresponding cumulative histogram. By using a logarithmic scale of conduction velocity it is possible to determine the relative effects of axotomy on the fast and slow conducting populations of fibers simply by examining the shifts in the conduction velocity distribution.

A parallel shift of the distribution to the left without a change in its shape would imply that both fast and slow conducting populations had slowed by the same relative amount. Differential effects would be apparent if the shift was not parallel. Vertical shifts in the distribution would indicate changes in the relative number of fibers conducting



at particular velocities. Such changes in the relative proportions of fast and slow conducting populations is exemplified in Figure 3. There is a relative reduction in the slow conducting population which is clearly evident in Figure 3C (the same plots are superimposed in Figure 8 (top)). It is not as easy though to estimate the magnitude of this reduction from the histograms of Figure 3B since the shapes of the control and axotomized conduction velocity distributions are different. For this reason cumulative histograms tend to make changes in the relative proportions of fast and slow conducting fibers more obvious.

In Figure 4 the cumulative conduction velocity distribution computed from the compound action potential of a control sural nerve is compared with that calculated by converting the cumulative fiber diameter histogram (obtained from histology done by J. Gillespie and B. Hanley) to a conduction velocity distribution. Scaling factors determined by Boyd and Kalu (1979) were used. Except for the slowest conduction velocities, the two conduction velocity distributions do not differ by more than 10%. Since histological counts grouped fibers into bins 2 microns wide, errors associated with the fiber diameter histogram could range from approximately  $\pm 5\%$  for the fastest conducting fibers to more than  $\pm 25\%$  for the slowest conducting fibers. The grouping of fibers into conduction velocity ranges for the computed conduction velocity distribution had a corresponding error of about  $\pm 5\%$  which varied little over



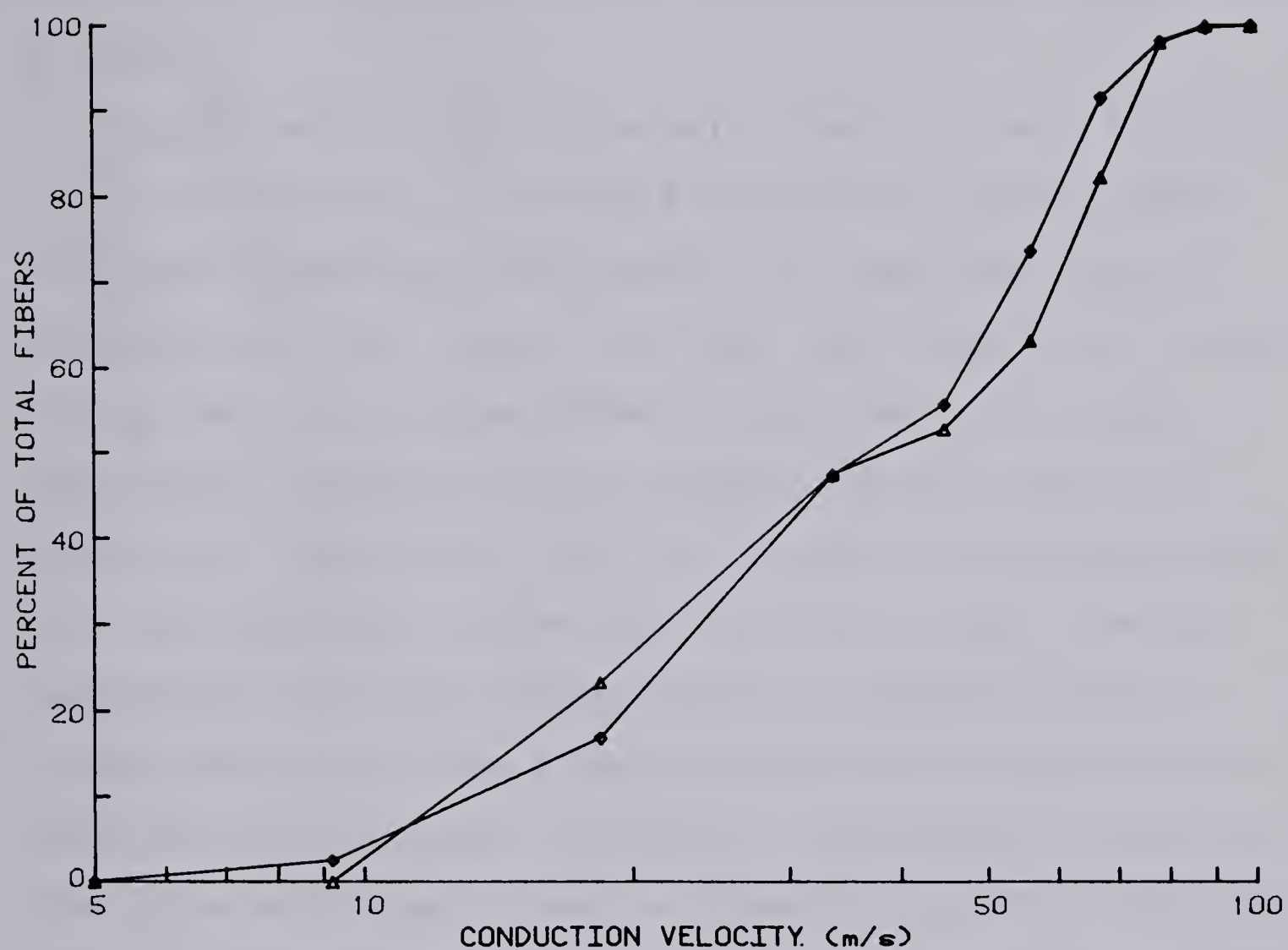


Figure 4

Comparison of a control sural nerve conduction velocity distribution obtained from the fiber diameter histogram ( $\diamond$ ) with that computed from the compound action potential ( $\triangle$ ).





the entire conduction velocity spectrum. The combined error arising from measurement of the conduction distance and variation in the shape of single unit potentials was at least  $\pm 5\%$ . Therefore, the two conduction velocity distributions agree relatively well within the limitations of error.

Approximately 200 single unit potentials were recorded from 5 sural nerves, 150 from 5 MG nerves in which dorsal roots were stimulated and another 150 from 4 MG nerves in which ventral roots were stimulated. Each population (single unit potentials recorded from a single nerve during one experiment) consisted of an average of 30-40 single unit potentials. Data points obtained for each nerve were plotted on a log-log scale and the best-fitting straight line was computed by the least-squares method. The amplitude and integrated areas of the single unit potentials were found to correlate well as power functions of the conduction velocity (the correlation coefficient was generally greater than 0.95 in the former case and greater than 0.85 in the latter). The single unit potential half-width (a measure of the duration) did not correlate as well, although the correlation coefficient was usually greater than 0.75.

The relationships obtained were thus of the form  $y = kv^n$ , where  $k$  is a constant,  $v$  the conduction velocity and  $n$  the slope of the line. The combined data for sural nerves are plotted in Figure 5, those for the MG dorsal root component in Figure 6 and for the MG ventral root component



in Figure 7. Regression parameters are listed in Table I.

No systematic variation with time after axotomy was apparent in the slopes of these relationships as determined from individual experiments. This was also evidenced by the fact that data points from various experiments, were distributed more or less uniformly about the regression lines.

Only sural single unit potentials were recorded over the full 273 day time course. Single unit potential recordings from the MG dorsal root component were restricted to 105 days and those for the ventral root component to 62 days. Since the slopes did not change systematically after axotomy, the same basic relationships for action potential generation and propagation were probably as valid for axotomized as for control nerves.

The fact that the correlation coefficients of the relationship between single unit potential amplitude and conduction velocity were so close to 1 also indicated that single unit potentials originating from the interior of the nerve trunk were not greatly attenuated (see also Stein & Oğuztöreli, 1978). A large amount of scatter would have been introduced if two single unit potentials with similar conduction velocities but different locations within the nerve trunk had been recorded with significantly different amplitudes.

Values of the slopes obtained from this analysis were used in computing the conduction velocity distribution.



Table I

Regression Parameters for Relationships between Single Axon Potentials and Conduction Velocity

Nerve	Dependent Variable	N	Coefficient log(k)± SE	k	Exponent n ± SE	Correlation Coefficient
Sural	Amplitude	194	-2.8186 ± 0.7007	0.001518	1.4796 ± 0.0349	0.9501
	Area	194	-2.7066 ± 0.8569	0.001966	1.0251 ± 0.0426	0.8655
	Half-width	194	0.0766 ± 0.7458	1.1929	-0.4368 ± 0.0371	0.6455
MG(s)	Amplitude	141	-3.4157 ± 0.6780	0.000384	1.7892 ± 0.0344	0.9749
	Area	141	-3.1182 ± 0.9203	0.000762	1.2080 ± 0.0467	0.9090
	Half-width	141	0.3538 ± 0.5830	2.2589	-0.6250 ± 0.0296	0.8718
MG(m)	Amplitude	147	-4.1704 ± 1.2134	0.000068	2.2707 ± 0.0595	0.9531
	Area	147	-4.0418 ± 1.2803	0.000091	1.8152 ± 0.0627	0.9223
	Half-width	147	0.1954 ± 0.5965	1.5682	-0.5155 ± 0.0292	0.8239

(N=number of cases, SE=standard error, s=sensory, m=motor)





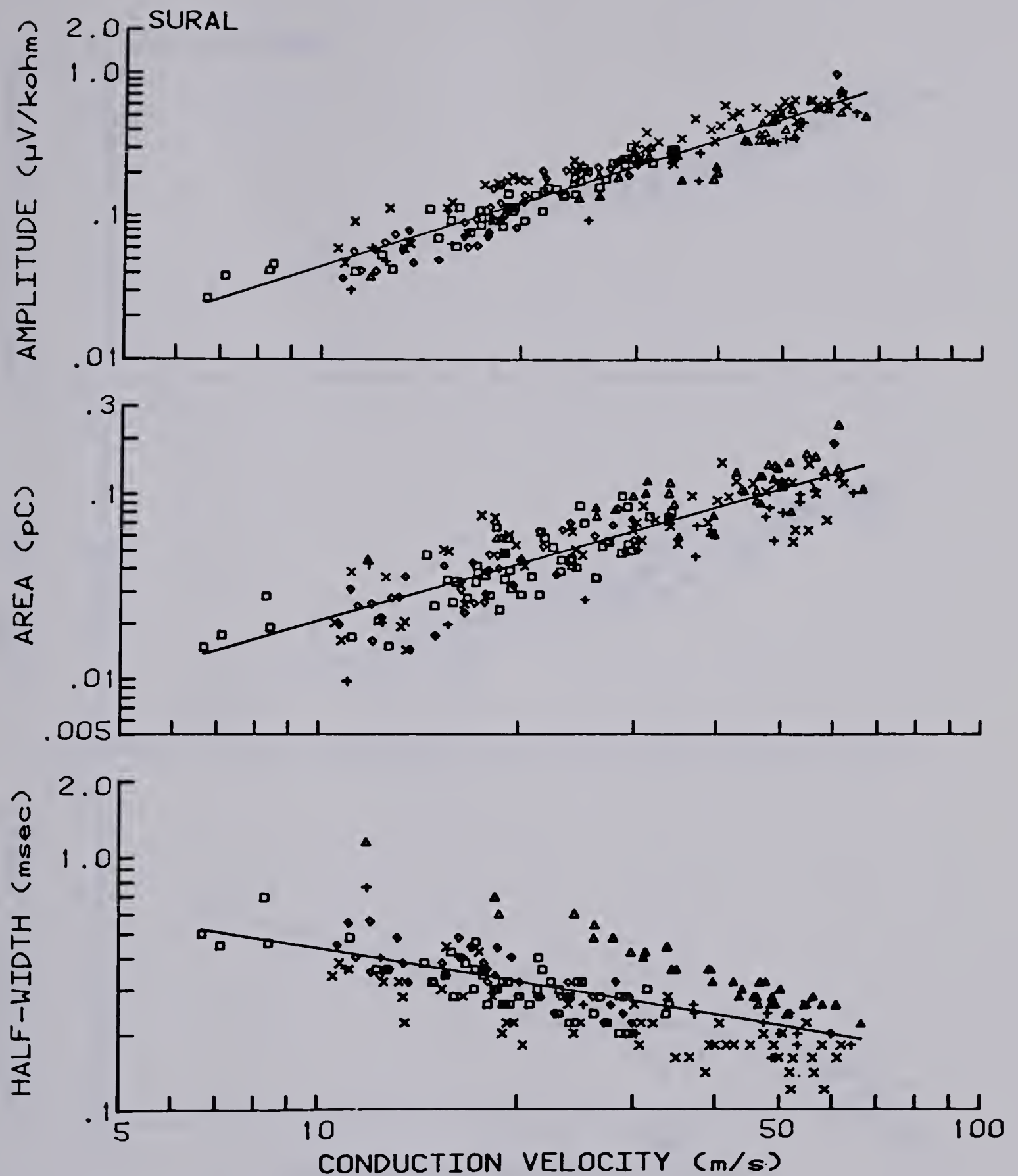


Figure 5

Single unit potential data recorded from sural nerve fibers 29 (+), 35 (Δ), 56 (X), 198 (□) and 273 (◇) days following axotomy plotted as  $y = kv^n$  on logarithmic coordinates. Regression parameters are listed in Table I.





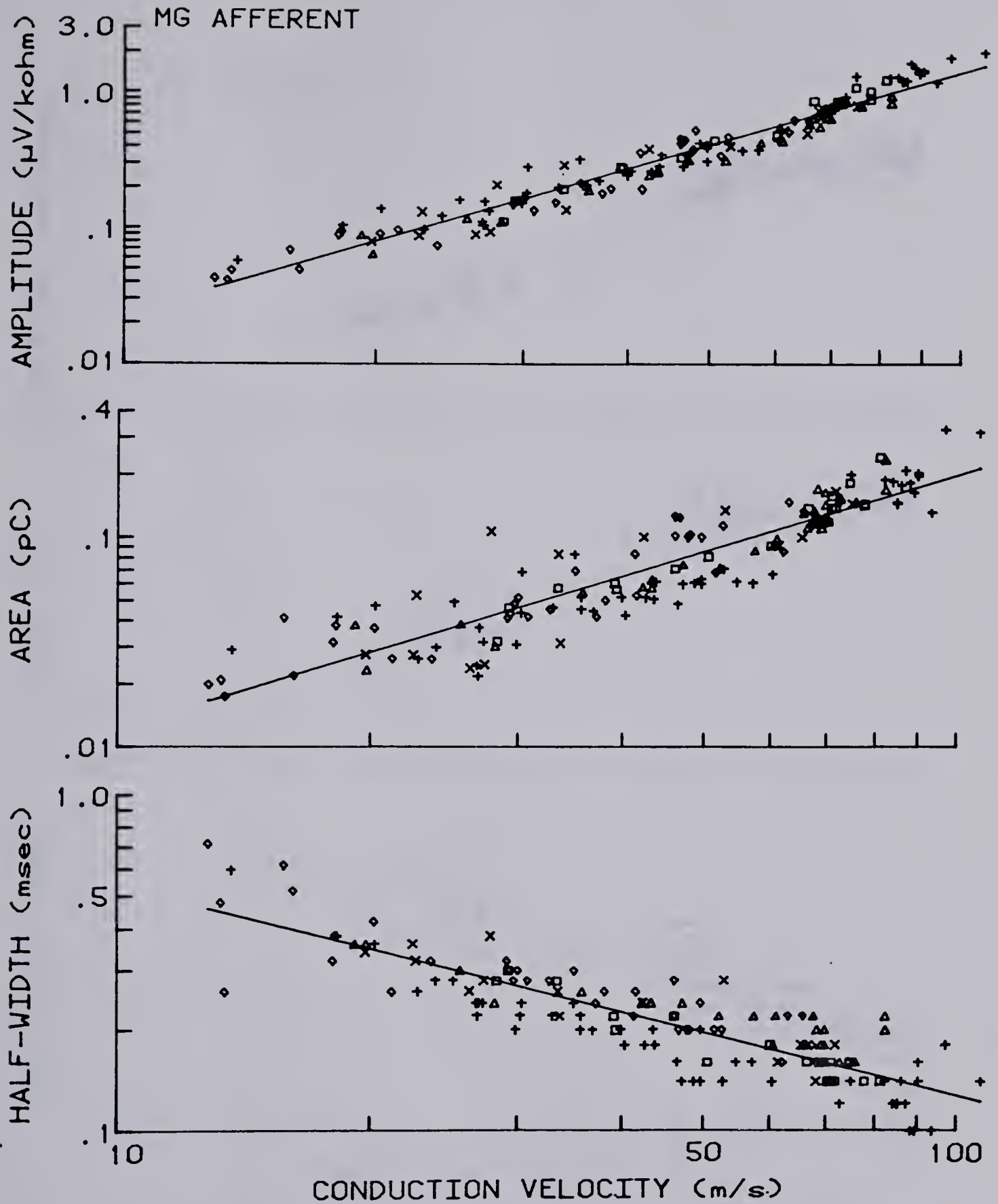


Figure 6

Single unit potential data recorded from MG afferent nerve fibers 0 (+), 29 ( $\square$ ), 35 ( $\triangle$ ), 71 ( $\times$ ) and 105 ( $\diamond$ ) days following axotomy plotted as in Figure 5. Regression parameters are listed in Table I.



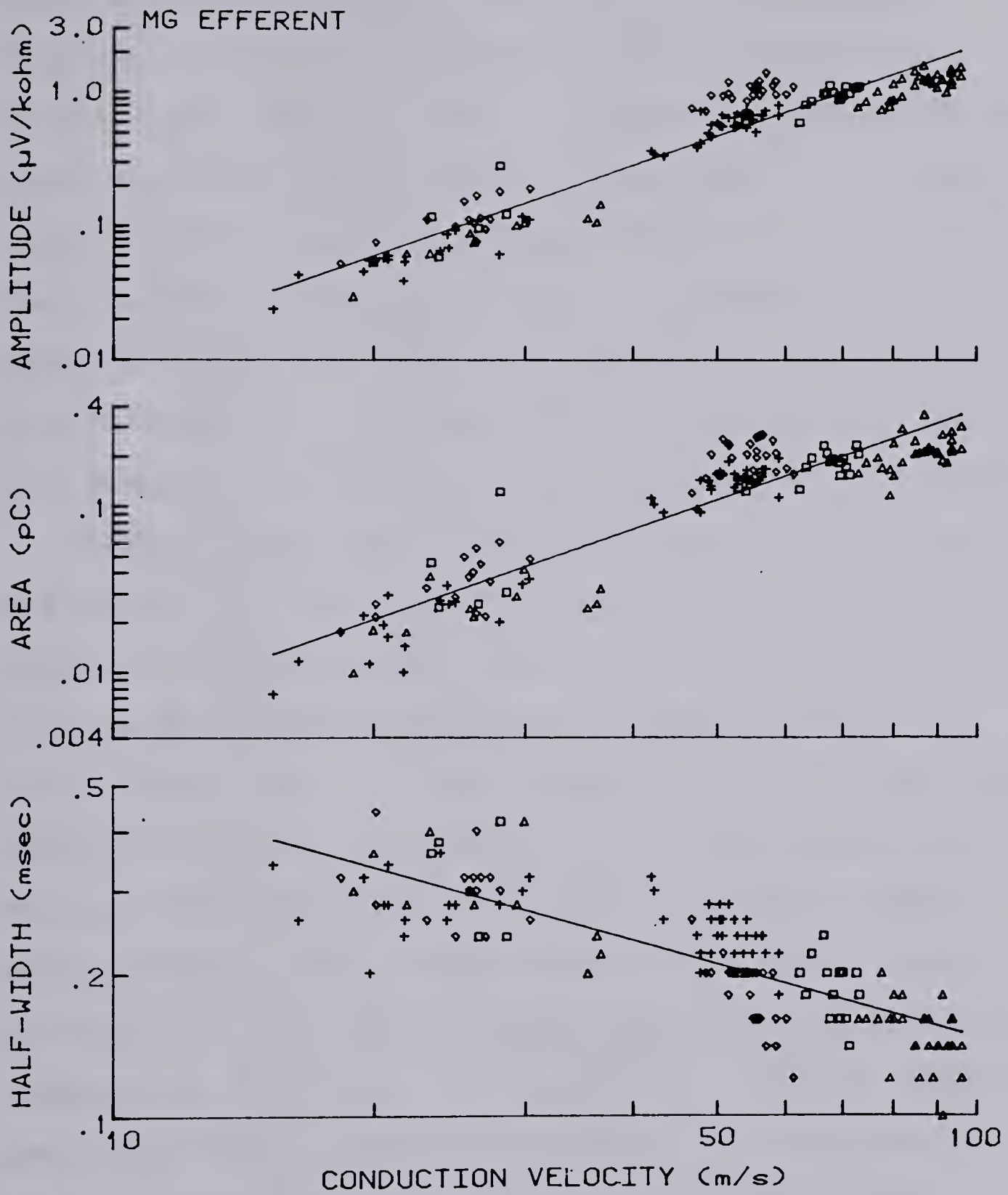


Figure 7

Single unit potential data recorded from MG efferent nerve fibers 0 ( $\Delta$ ), 34 ( $\diamond$ ), 62 (+) and 71 ( $\square$ ) days following axotomy plotted as in Figure 5. Regression parameters are listed in Table I.



Conduction velocity distribution values were normalized, scaled by the  $n$ th power of the conduction velocity (where  $n$  is the slope obtained from the relationship between integrated single unit potential area and conduction velocity) and summed in order to obtain the compound action potential charge value expected from a particular conduction velocity distribution. The actual charge decline as recorded from axotomized nerves could then be compared with the expected decline resulting from changes in the conduction velocity distribution alone, making the assumption that the total number of conducting fibers had remained unchanged.

Control sural nerve conduction velocity distributions were bimodal in nature as indicated by the plateau in the conduction velocity distribution of Figure 3. Within the first month following axotomy the conduction velocity distribution lost its bimodal shape (Figure 8). There was a slowing of the fast conducting fibers and an apparent loss of slow conducting fibers since their relative numbers decreased below that of the control conduction velocity distribution. The differences may have been exaggerated by a tendency for the single unit potentials recorded from slow conducting fibers to be diphasic even under monophasic recording conditions (Blair & Erlanger, 1933). Slow conducting fibers sometimes had a substantial negative phase as illustrated in Figure 2. Fast conducting fibers showed relatively less negativity. As a result, there may have been some cancellation of positive and negative phases among slow





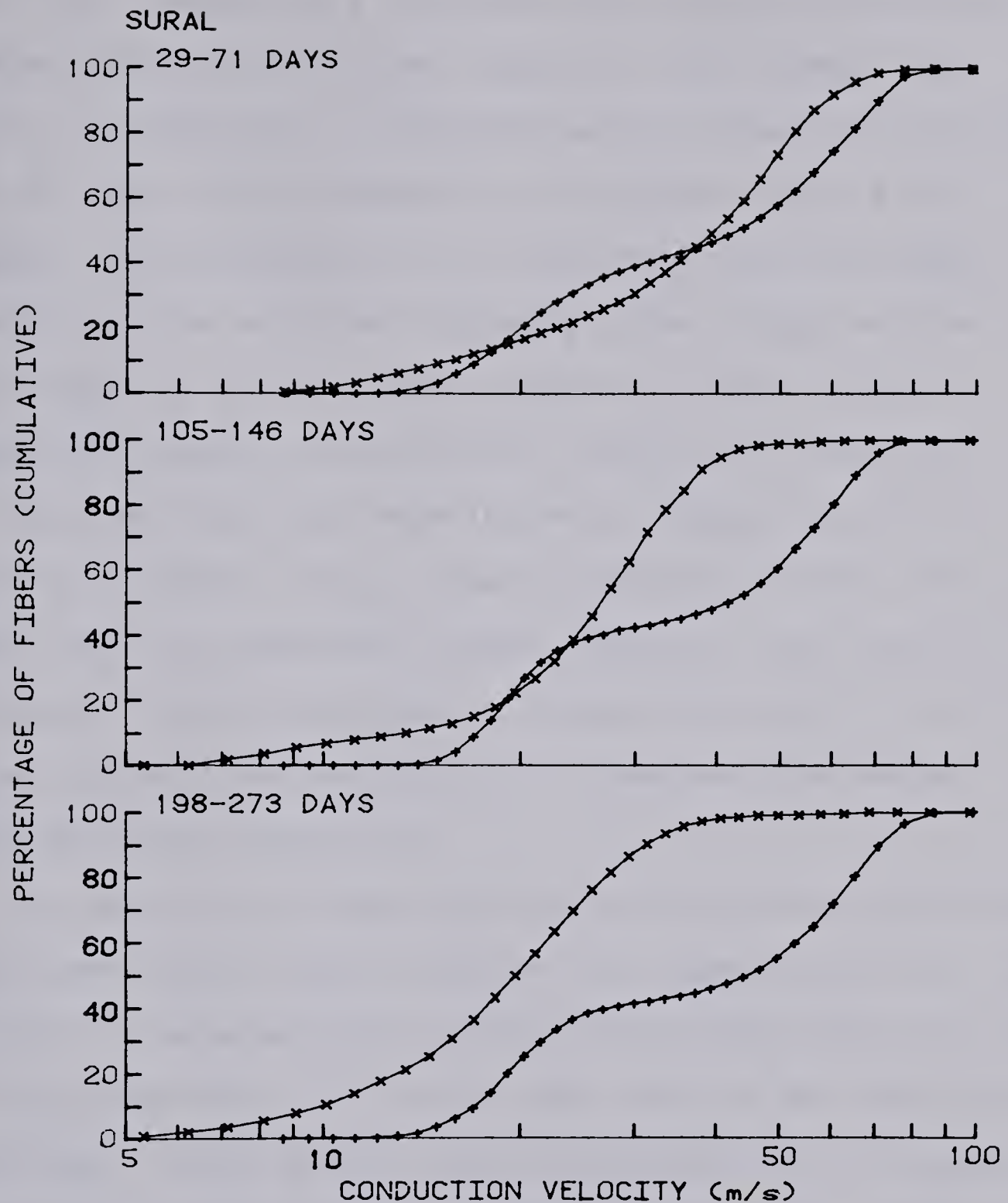


Figure 8

Progressive changes in the conduction velocity distribution of sural nerves following axotomy. Conduction velocity distributions for axotomized nerves (X) examined in the indicated time periods were averaged and plotted together with the averaged conduction velocity distributions of corresponding control nerves (+). Refer to text for discussion.



conducting fibers of slightly different conduction velocities, producing a compound action potential which underestimated the relative number of slow conducting fibers. A comparison of compound action potentials recorded from the nerve when stimulating the dorsal roots with compound action potentials recorded from the roots when stimulating the nerve peripherally, also suggested that there might be too few slow conducting fibers in the conduction velocity distribution. Conduction velocity distributions computed from the root compound action potentials did not always show a reduction in the relative number of slow conducting fibers. However, this was not a consistent finding nor does it necessarily conflict with the conduction velocity distributions computed from nerve compound action potentials.

The spacing between recording and reference electrodes on the roots was slightly greater (by approximately 2-3 mm) than on the nerve and the temperature of the spinal paraffin pool was generally  $1^{\circ}$ - $2^{\circ}$  lower than that of the body and the muscle pool. Both factors would contribute to an increase in the duration of single unit potentials (Paintal, 1966, Stein & Pearson, 1971). The lower spinal temperature would also tend to slow single unit conduction velocity slightly. Consequently, the compound action potentials recorded from the roots would appear to have a relatively larger contribution from slow conducting fibers than the potentials recorded from the nerve. Considering further that the single



unit templates used to compute the dorsal root conduction velocity distributions were recorded from the nerve, some caution should be exercised in evaluating the importance of this result. Either way though, the conduction velocity distributions became unimodal following axotomy, implying that the fast conducting fibers initially slowed relatively more than the slow conducting fibers and hence filled in the original 'gap' in the bimodal conduction velocity distribution.

With increasing time following axotomy there was a progressive decrease in the conduction velocities of all nerve fibers (Figure 8). The decline was quantified for fast conducting fibers and slow conducting fibers respectively by determining the conduction velocities below which 80% and 20% of the total number of fibers were represented in the conduction velocity distribution. An estimate of their initial rates of decay following axotomy was obtained by fitting the data with an exponential decay curve of the form  $v = v_0 e^{-t/T}$  where  $v_0$  is the control conduction velocity and  $T$  the rate constant. Fitting the points with a curve of the form  $v = v_1 e^{-t/T} + v_2$ , where  $v_1 + v_2$  is the control conduction velocity and  $v_2$  the asymptotic value, gives an estimate of the endpoint of the decay process (Figure 9). Regression curves were calculated using all data points, but for the sake of clarity only the averages of groups of points (grouped into the same time intervals as Figures 8, 10 and 11) have been plotted in Figure 9. The method of obtaining





the regression curves is described in Appendix II.

It was felt that curves of the form  $v = v_0 e^{-t/T}$  gave a better estimate of  $T$  than those of the form  $v = v_1 e^{-t/T} + v_2$  since the latter required the introduction of a third parameter  $v_2$  which influenced the accuracy with which  $v_1$  and  $T$  could be determined. Furthermore,  $v_2$  is really the limit of the conduction velocity as  $t$  becomes very large. Since the range of observations extended only to 273 days the conduction velocities may have declined further had the nerves remained in their axotomized state for a longer period of time. Values of the regression parameters are listed in Table II.

The conduction velocity of the fast conducting fibers declined significantly faster than that of the slow conducting fibers ( $t$ -test,  $2P < 0.001$ ). However, while the fast conducting fibers had an asymptotic conduction velocity  $v_2$  which was significantly greater than zero ( $t$ -test,  $P < 0.0005$ ), the slow conducting fibers tended to slow to a final velocity of zero. A systematic underestimate of the relative number of slow conducting fibers following axotomy would probably have reduced the 20% conduction velocities relatively more as time progressed, therefore causing both the time constant and the asymptotic value to be underestimated. The computed time constant was already so great that it was beyond the period of the experimental observations so it cannot be concluded that these fibers actually all died or stopped conducting.





Table II

Regression Parameters for Conduction Velocity Decay Curves

Nerve	Fiber Type	N	Control Velocity (m/s) $\log(v_0) \pm SE$	$v_0$	Rate Constant (days) $T \pm SE$	Asymptotic Velocity (m/s) $v_2 \pm SD$
Sural	Slow	36	$1.3168 \pm 0.0829$	20.74	$556 \pm 101$	$20.55 \pm 4.98$
	Fast	36	$1.7946 \pm 0.0517$	62.32	$264 \pm 14$	$37.54 \pm 4.99$
MG(s)	Slow	34	$1.4469 \pm 0.1413$	27.98	$424 \pm 107$	$56.74 \pm 3.80$
	Fast	34	$1.9681 \pm 0.0645$	92.92	$249 \pm 17$	
MG(m)	Slow	30	$1.4496 \pm 0.1688$	28.18	$973 \pm 761$	$56.74 \pm 3.80$
	Fast	30	$1.9529 \pm 0.0768$	89.72	$400 \pm 59$	
Nerve	Fiber Type	N	Control Velocity (m/s) $(v_1+v_2) \pm SD$		Rate Constant (days) $T \pm SD$	
Sural	Fast	36	$63.87 \pm 6.99$		$119 \pm 30$	
MG(s)	Fast	34	$97.14 \pm 7.16$		$73 \pm 16$	
MG(m)	Fast	30	$95.97 \pm 5.67$		$38 \pm 12$	

(N=number of cases, SE=standard error, SD=standard deviation, s=sensory, m=motor)



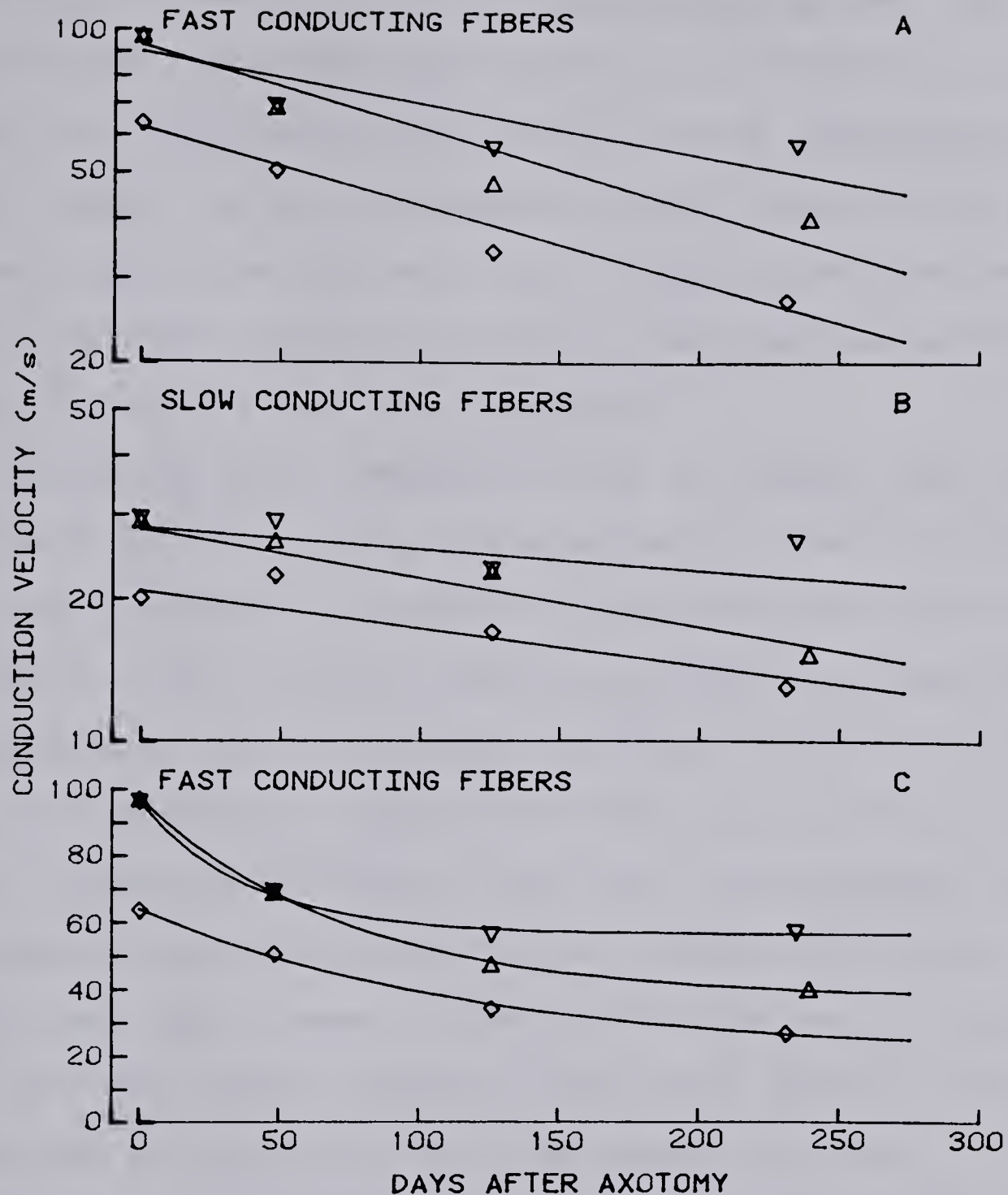


Figure 9

Conduction velocity decay curves. A and B. Plots of  $v = v_0 e^{-t/T}$  on a semi-log scale for fast and slow conducting fibers: sural (◇), MG sensory (△) and MG motor (▽). Each point represents the mean from several experiments. C. Plots of  $v = v_1 e^{-t/T} + v_2$  on a linear scale for fast conducting fibers. The latter are not shown for slow conducting fibers since  $v_2$  was zero, i.e., the decay curves could only be formulated in one way. Note that the decay of fast afferent fibers is faster than in any of the other cases. Regression parameters for these curves are listed in Table II.



On the other hand, if a significant number of slow conducting fibers did in fact stop conducting very soon after axotomy, the 20% level could have shifted to a higher conduction velocity than the control value. Subsequently, fibers conducting at intermediate velocities would have been represented at the 20% level and it would have been their rate of decline rather than that of the slow conducting fibers that would have been measured.

The MG nerve was separated into its sensory and motor components by stimulating either dorsal or ventral roots. The control conduction velocity distribution of the sensory component, like the sural nerve, was bimodal although the plateaus were less pronounced than those of control surals. The fast conducting fibers of the MG afferents were, of course, faster than those of the sural. The tendency toward a unimodal conduction velocity distribution following axotomy was much slower in the MG than the sural (Figure 10). This may simply reflect a relatively greater difference between MG afferent fast and slow conducting fiber velocities since the corresponding rates of conduction velocity decline did not differ significantly from those of the sural. The same progressive reduction of conduction velocity for all fibers as in the sural was evident in the MG. The fast conducting fibers slowed significantly faster than the slow conducting fibers (t-test,  $2P < 0.02$ ) but approached an asymptotic value which was significantly greater than zero (t-test,  $P < 0.0005$ ), while the final value





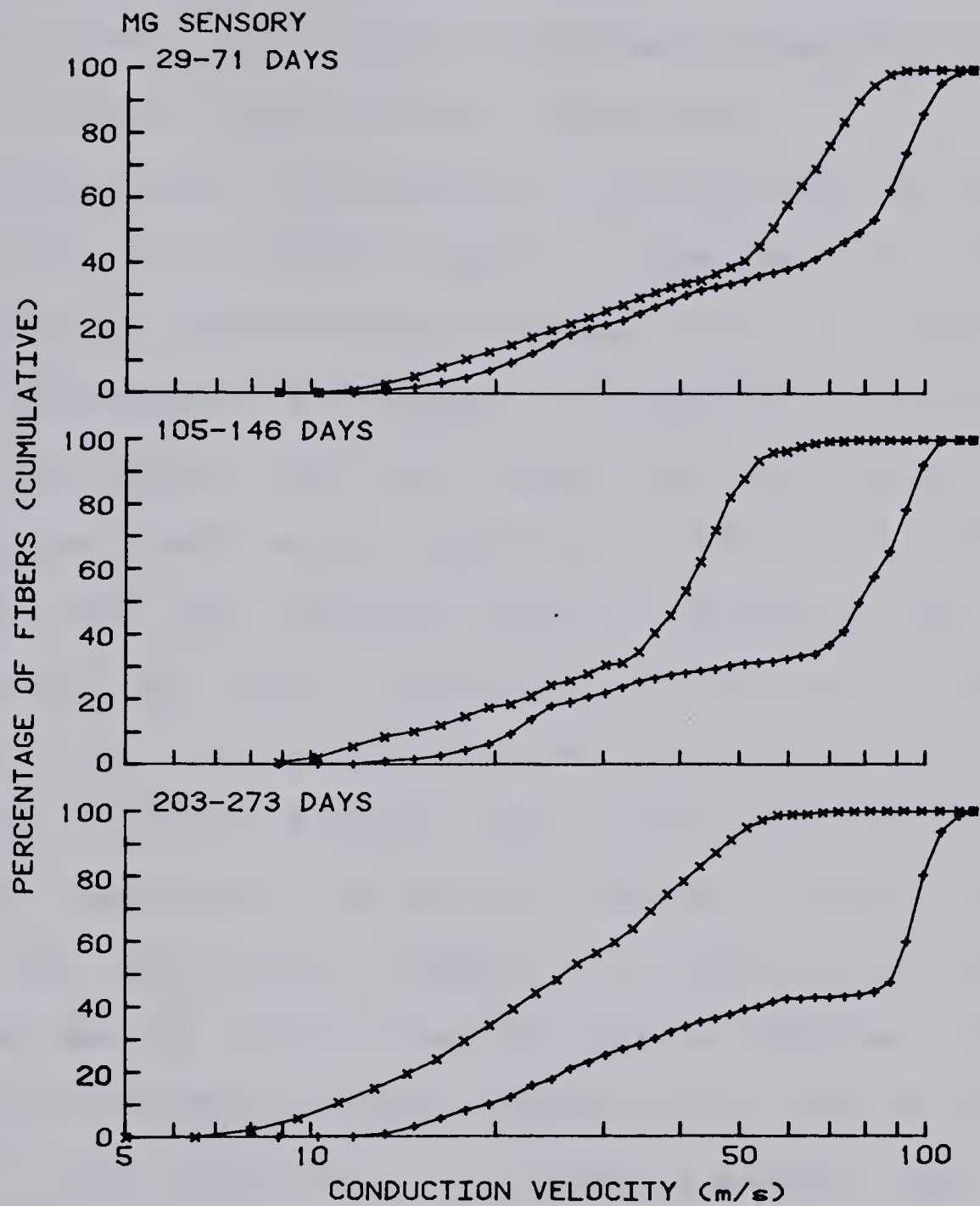


Figure 10

Progressive changes in the conduction velocity distribution of MG nerve sensory components following axotomy. Conduction velocity distributions are plotted as in Figure 8. Refer to text for discussion.



projected for slow conducting fiber conduction velocity was zero.

The MG efferent fibers presented a different picture. While the conduction velocity distribution was distinctly bimodal (a clear separation of alpha- and gamma-motoneurons), the nature of the distribution did not change following axotomy (Figure 11). Because the difference in conduction velocities was so great, the fast conducting fibers approached their asymptotic conduction velocity before they reached the slow conducting fiber range. Furthermore, there was no significant difference in the rate constants for the conduction velocity decline of fast and slow conducting fibers. The asymptotic velocity of MG efferent fast conducting fibers was significantly greater than that of the MG afferent fast conducting fibers (t-test,  $2P < 0.005$ ) confirming the earlier finding of Höffer et al. (1979) that the fastest conducting afferent fibers were affected more by axotomy than the fastest efferent fibers. The rate of slowing was also significantly less in efferent fibers (t-test,  $2P < 0.005$ ). It therefore appears that degeneration progresses faster and may also continue longer in fast conducting afferent fibers than in alpha-motoneurons.

There was considerably more scatter in the range of conduction velocities for the 20% level of efferent fibers than afferent fibers. As a result, the rate of conduction velocity decline was not significantly different from zero.



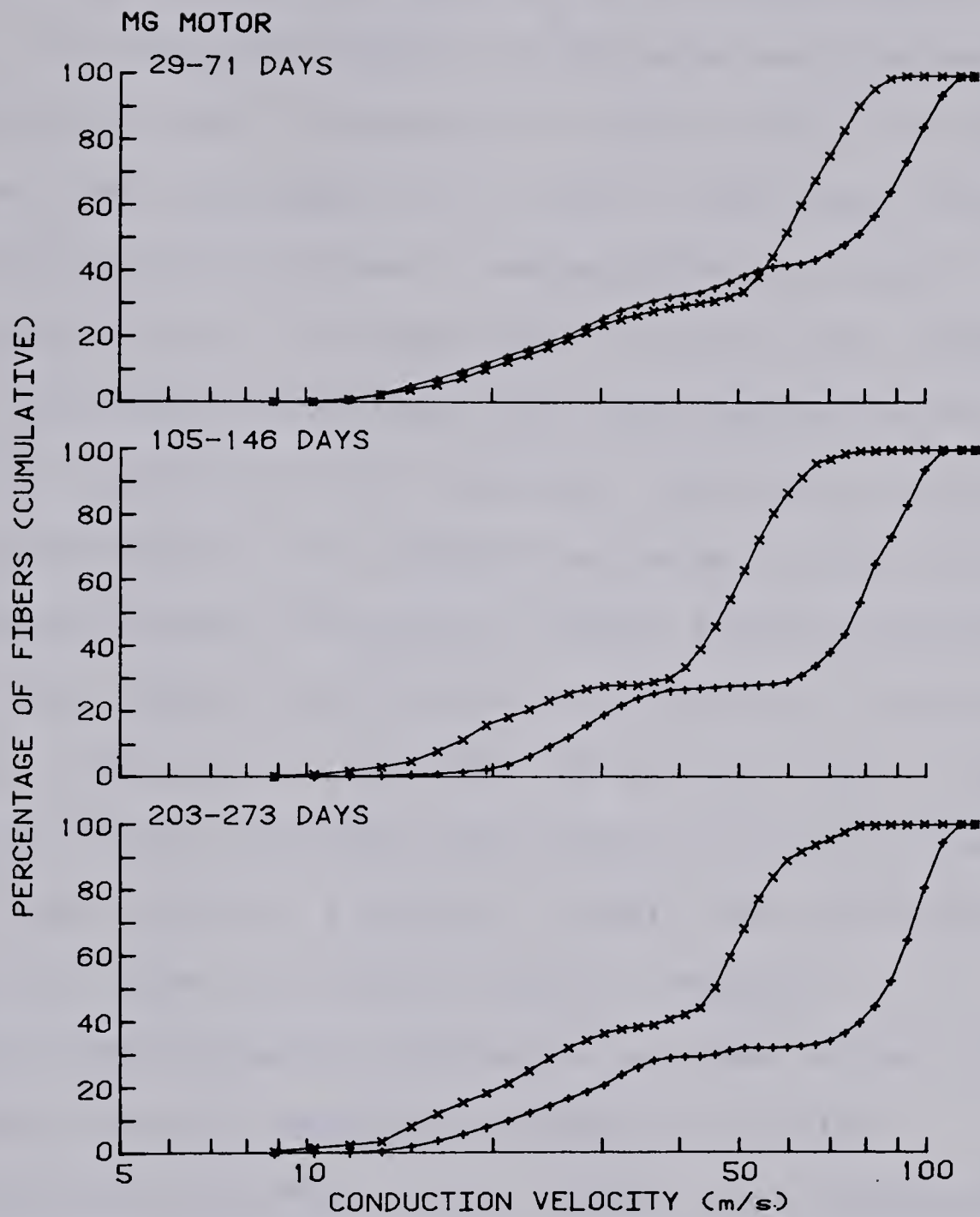


Figure 11

Progressive changes in the conduction velocity distribution of MG nerve motor components following axotomy. Conduction velocity distributions are plotted as in Figure 8. Refer to text for discussion.





Due to the difficulty in denervating all tail and gluteal muscles, a few usually remained innervated, resulting in an EMG artifact which was recorded when stimulating the ventral roots. In a few experiments the MG nerve was crushed after recording in order to measure the EMG artifact in isolation. This artifact was opposite in sign to the neural potential and occurred with a latency corresponding to that of gamma-motoneurons. Although small, the artifact tended to reduce the slow conducting fiber contribution to the motor compound action potential somewhat. The effect was probably more substantial on the conduction velocity distributions of axotomized nerves than control nerves since concomitant with conduction velocity decline was a reduction in single unit potential amplitude. Thus, the EMG artifact would reduce the compound action potential contribution of these slower conducting fibers to a greater extent than the faster conducting fibers of control nerves. Whether gamma-motoneurons were affected to a lesser extent than slow afferent fibers is therefore difficult to infer.

As noted by Hoffer et al. (1979), the integrated area under a compound action potential (referred to as charge because of its dimensions) was dramatically reduced following axotomy. However, it proved to be less straightforward to quantify compound action potential charge decay than conduction velocity decline. There was inevitably some progressive deterioration of compound action potentials during recording which could produce a reduction in





amplitude without significantly altering the shape. Consequently, it was possible to extract information about changes in the relative distribution of conduction velocities (determined by the shape of the compound action potential) more reliably than changes in the absolute number of conducting fibers (determined by the magnitude of the compound action potential). Moreover, the absolute number of axons and hence the magnitude of the compound action potential varied from preparation to preparation.

Analysis similar to that for conduction velocity was carried out for compound action potential charges recorded both from the spinal roots and the peripheral nerves. Charge was plotted against time after axotomy and the values were fitted with curves of the form  $Q = Q_0 e^{-t/T}$  and  $Q = Q_1 e^{-t/T} + Q_2$ , where  $Q_0$  and  $Q_1 + Q_2$  are the control charge values and  $Q_2$  is the asymptotic charge value (Table III).

Comparison of the MG sensory and motor compound action potentials as recorded from the dorsal and ventral roots indicated a significant difference in the rates of decay (t-test,  $2P < 0.01$ ), the sensory compound action potential charge declining faster than that of the motor compound action potential (results for root charges were combined with the results obtained by Hoffer et al. (1979) in Figure 12). Surprisingly though, there was no significant difference in the rates of decay as determined from nerve compound action potentials. From the relative changes in afferent and efferent conduction velocities, a faster rate



Table III

Regression Parameters for Compound Action Potential Charge Decay Curves

Nerve	Potential Type	N	Control Charge (pC) $\log(Q_0) \pm SE$	Rate/Constant (days) $T \pm SE$	
Sural	Root	33	1.8463 $\pm$ 0.1746	180 $\pm$ 23	
	Nerve	34	1.9119 $\pm$ 0.2087	155 $\pm$ 21	
	Computed	36	81.64*	313 $\pm$ 19	
MG(s)	Root	33	1.7792 $\pm$ 0.2015	137 $\pm$ 14	
	Nerve	33	1.4255 $\pm$ 0.2825	142 $\pm$ 26	
	Computed	34	26.64*	221 $\pm$ 15	
MG(m)	Root	35	2.2216 $\pm$ 0.1720	217 $\pm$ 30	
	Nerve	32	2.0485 $\pm$ 0.1932	149 $\pm$ 23	
	Computed	30	111.81*	246 $\pm$ 41	
Nerve	Potential Type	N	Control Charge (pC) $(Q_1+Q_2) \pm SD$	Rate Constant (days) $T \pm SD$	Asymptotic Charge (pC) $Q_2 \pm SD$
Sural	Root	33	78.58 $\pm$ 13.17	62 $\pm$ 29	21.98 $\pm$ 9.02
	Nerve	34	88.95 $\pm$ 54.66	124 $\pm$ 123	7.73 $\pm$ 38.90
	Computed	36	88.95 $\pm$ 24.50*	195 $\pm$ 86	22.09 $\pm$ 17.46
MG(s)	Root	33	65.52 $\pm$ 13.38	83 $\pm$ 38	9.58 $\pm$ 9.20
	Nerve	33	32.93 $\pm$ 5.03	31 $\pm$ 15	7.85 $\pm$ 3.36
	Computed	34	32.93 $\pm$ 1.14*	93 $\pm$ 32	9.87 $\pm$ 3.33
MG(m)	Root	35	183.95 $\pm$ 26.16	52 $\pm$ 28	69.09 $\pm$ 17.52
	Nerve	32	133.51 $\pm$ 16.90	24 $\pm$ 12	37.58 $\pm$ 11.28
	Computed	30	133.51 $\pm$ 22.87*	54 $\pm$ 30	54.23 $\pm$ 15.69

\*Initialized to control nerve values  
(N=number of cases, SE=standard error, SD=standard deviation, s=sensory, m=motor)



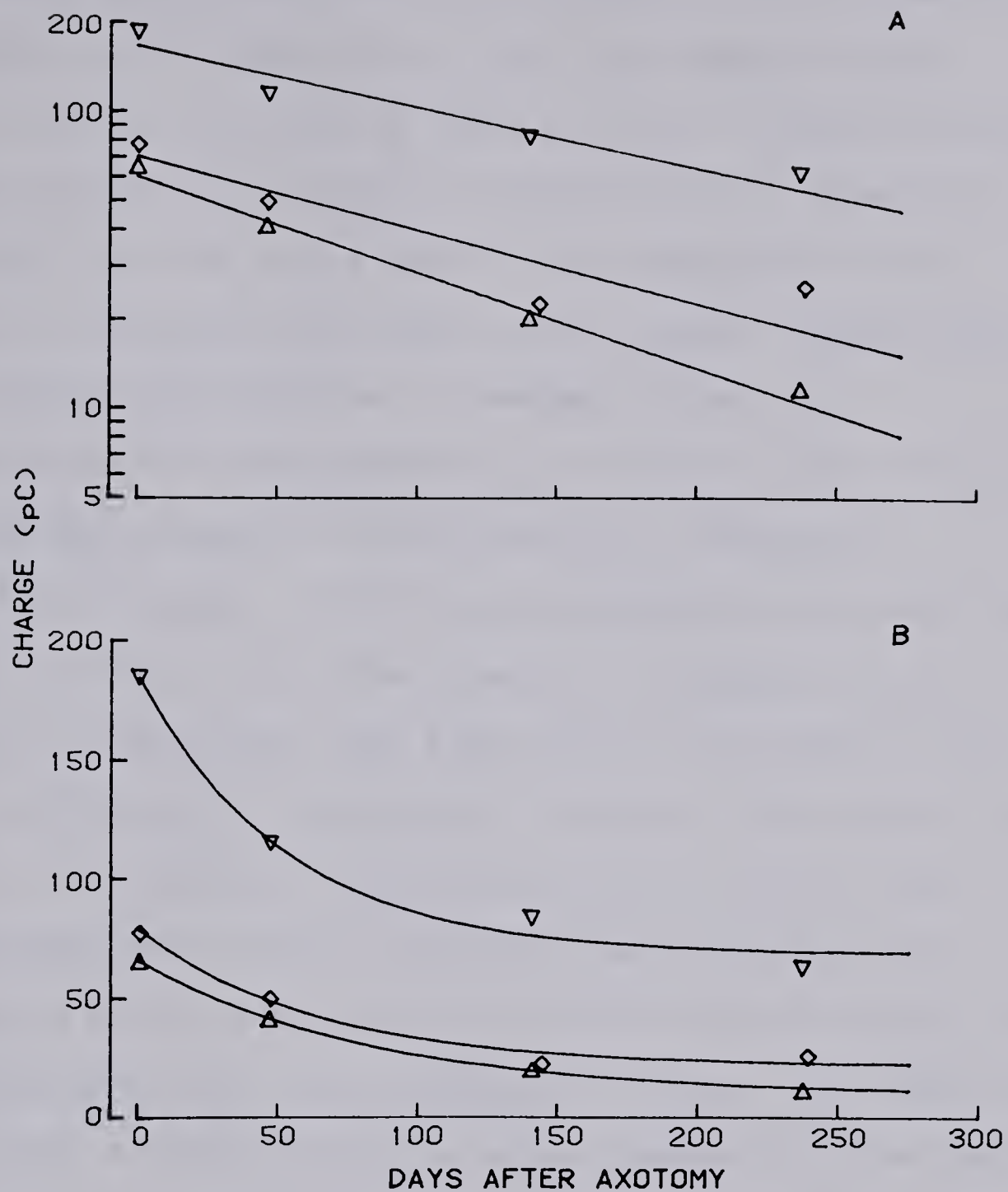


Figure 12

Charge decay curves for compound action potentials recorded from the spinal roots. A. Plots of  $Q = Q_0 e^{-t/T}$  on a semi-log scale for compound action potentials recorded from L7 and S1 dorsal roots while stimulating the sural ( $\diamond$ ) or MG ( $\Delta$ ) nerves and from the ventral roots while stimulating the MG nerve ( $\nabla$ ). Each point represents the mean from several experiments. Note that the decay of MG sensory charge is faster than MG motor charge. B. Plots of  $Q = Q_1 e^{-t/T} + Q_2$  on a linear scale. Note that MG motor charge asymptotes to a higher level relative to its control than MG sensory charge. Regression parameters are listed in Table III.





of charge decay would have been expected for the sensory compound action potentials. This discrepancy may be reconciled by considering the fact that a faster rate of decay was seen in the motor compound action potential recorded from the nerve than in the compound action potential recorded from the ventral roots, suggesting that the charge recorded from axotomized nerves was underestimated. One possibility is that the EMG artifact reduced the compound action potential charge by a significant amount, affecting axotomized nerves more than control nerves. Since the asymptotic compound action potential charge was less than 40% of the control value, an EMG artifact which reduced the charge on the control nerve by 10%, for example, could have reduced that of the axotomized nerve by 25%. Such an underestimation is supported by the fact that no significant difference was found between the rates of decay of dorsal roots and nerve for either the MG sensory or sural compound action potential charges; i.e., it is therefore unlikely that there should have been a significant difference in the case of the MG motor and ventral root compound action potentials.

The rate of charge decline of sural compound action potentials did not differ significantly from the corresponding rates of either MG sensory or motor compound action potential charges whether recorded from the spinal roots (Figure 12), or the nerve (Figure 13). Although not significantly different, the rate of sural charge decay was



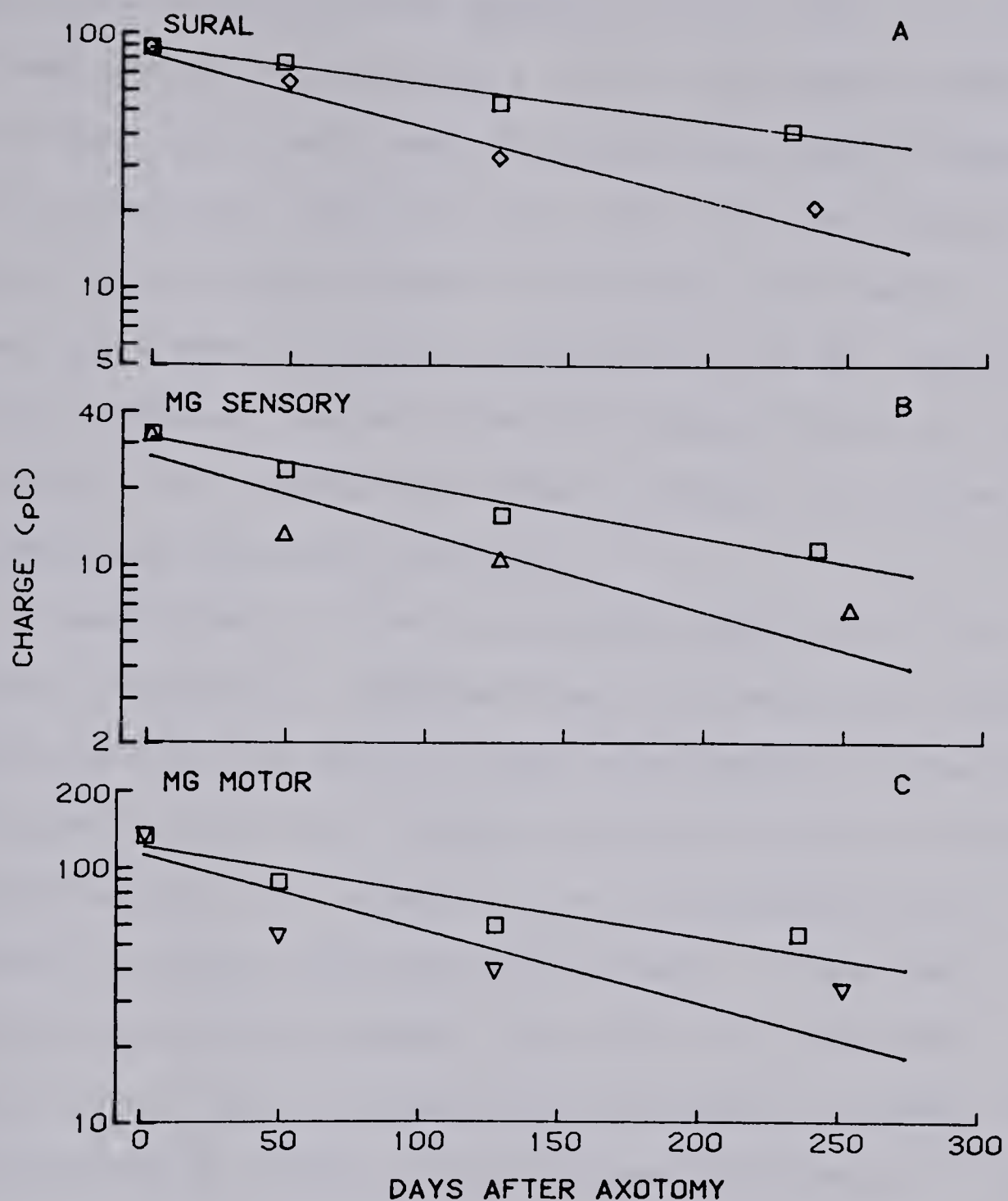


Figure 13

Decay curves of the form  $Q = Q_0 e^{-t/T}$  for compound action potential charge recorded from nerves compared with the charge expected from the computed conduction velocity distributions. A. Charge from sural compound action potentials ( $\diamond$ ) and corresponding expected charge values which have been initialized to control sural values ( $\square$ ). B. Charge from MG sensory compound action potentials ( $\Delta$ ) and expected charge ( $\square$ ). C. Charge from MG motor compound action potentials ( $\nabla$ ) and expected charge ( $\square$ ). Points are plotted as in Figure 12A. Note that the difference between the slopes of recorded and expected charge is similar for all cases. Regression parameters are listed in Table III.



slower than that of the MG sensory charge. This is probably a consequence of there being a relatively larger number of slow conducting fibers contributing to the sural compound action potential, along with the fact that the conduction velocity difference between the fastest and slowest conducting fibers is not as great as in the MG. The decline of sural compound action potential charge therefore reflects the rate of fast conducting fiber slowing to a lesser extent than does the MG sensory charge.

As mentioned earlier an expected compound action potential charge was computed from the conduction velocity distribution on the basis of the relationship between single unit potential area and conduction velocity. By fitting the computed values with a decay curve the expected rate constant of charge decay was determined. It was thus possible to estimate whether the shift in conduction velocity distribution alone could completely account for the decreased charge values. A significant difference in the rate constants of recorded and computed charge decay would indicate that other factors had contributed as well.

There was a difference between these two rate constants in all cases (Figure 13), the recorded charge decaying at a faster rate than the computed charge. Except for the MG sensory compound action potential charge, the difference was significant (t-test,  $2P < 0.001$  (sural),  $2P < 0.05$  (MG motor),  $0.05 < 2P < 0.1$  (MG sensory)). It would have been significant there as well, had there been slightly less variability in





the recorded compound action potential charge.

The discrepancy between the two rate constants must be interpreted as a loss in conducting fibers following axotomy, although the extent of such a loss may have been exaggerated by factors which tended to alter the amplitude or shape of the compound action potential. At least part of the difference in the case of the MG motor component may have been due to EMG artifact. Its effects could have been twofold--first, to reduce the recorded charge as explained above, and second, to weight the conduction velocity distribution more heavily in favor of fast conducting fibers. Since the computation of expected compound action potential charge assumed that the total number of conducting fibers remained constant, an underestimation in the relative number of slow conducting fibers (due to partial cancellation of their contribution to the compound action potential by the EMG artifact) would have meant that more fast conducting fibers were contributing to the computed compound action potential charge. This would have artificially increased the charge values, particularly for axotomized nerves and thereby led to an underestimation of the actual rate of charge decay.

A significant difference between the computed charge and the charge recorded from axotomized nerves could have occurred in two ways. Fibers may have stopped conducting as the result of degenerative changes following axotomy or they may have stopped conducting as the result of trauma suffered





during preparation for recording. Changes definitely did occur while recording from the nerves since compound action potential charge was sometimes reduced by as much as 20-30% over periods of 15-30 minutes. This was presumably due to loss of axoplasm from the cut nerves combined with concentration changes in the intracellular space and the restricted extracellular space formed by bringing the nerves into paraffin oil for recording. The nerves were ligated to minimize these changes and the compound action potentials generally stabilized, remaining relatively constant for hours afterward.

The decline of charge during the course of recording compound action potentials occurred in both control and axotomized nerves to more or less the same degree. Therefore, the rate constants of the exponential charge decay should not have been altered significantly. Based on this assumption, it must be concluded that a significant number of fibers stopped conducting in response to axotomy, although the fact that the recorded nerve charge values appear to reach non-zero limits (Figure 14) implies that a certain population of fibers retain the ability to conduct action potentials, perhaps indefinitely. It is interesting to note that the difference between the rates of recorded and computed charge decay are nearly the same for MG efferent and afferent fibers, indicating that during the initial stages of degeneration approximately the same percentage of fibers stopped conducting in both cases.



Charge decay did not continue at its initial rate since there there was a tendency for the charge to approach asymptotic limits. Therefore, it was difficult to estimate the actual percentage of fibers lost. Based on the asymptotic values it would appear though, that it was no more than 20-30%.



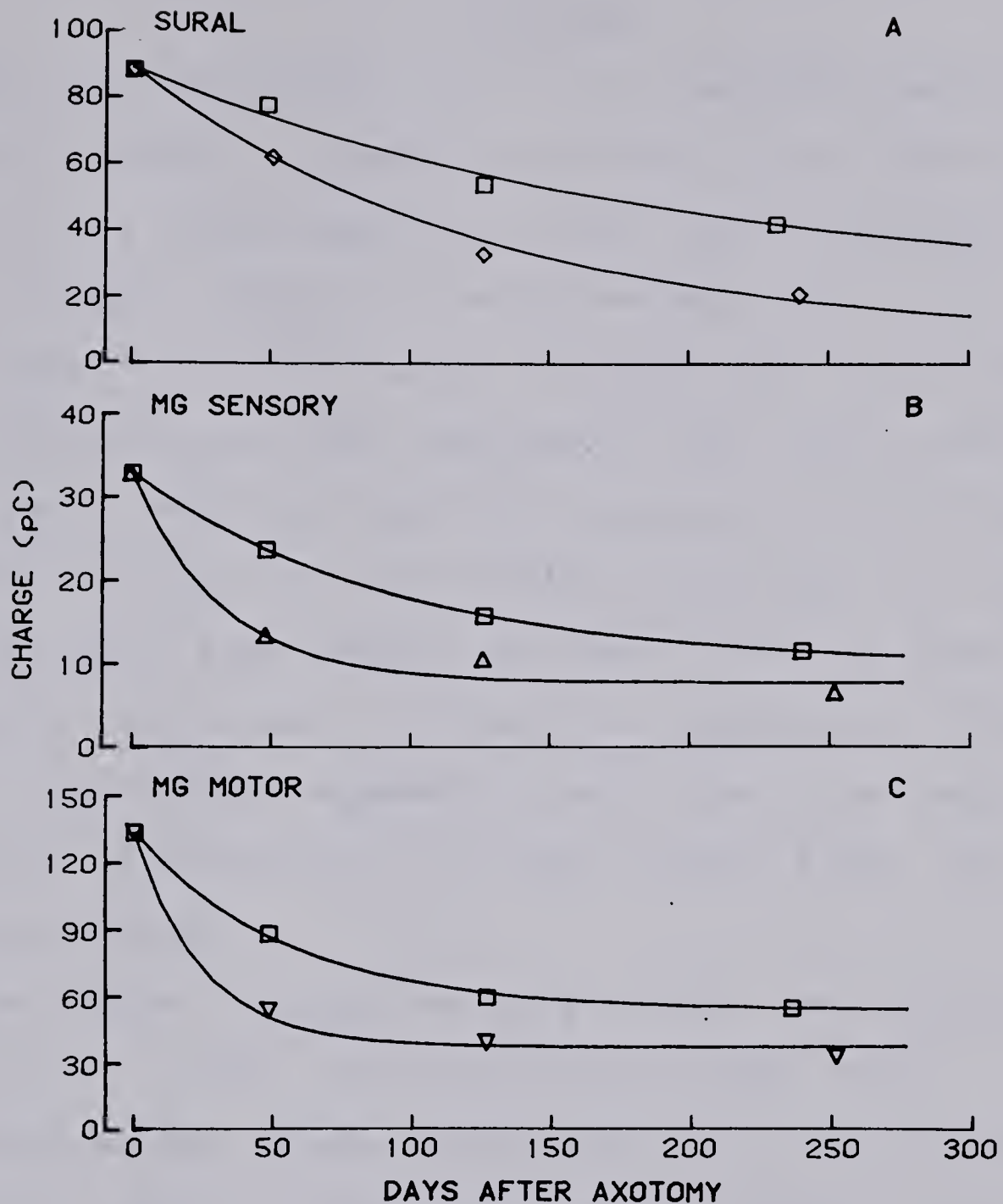


Figure 14

Decay curves of the form  $Q = Q_1 e^{-t/T} + Q_2$  for compound action potential charge recorded from the nerves compared with the charge expected from the computed conduction velocity distribution. A. Charge from sural compound action potentials ( $\diamond$ ) and corresponding expected charge values which have been initialized to control sural values ( $\square$ ). B. Charge from MG sensory compound action potentials ( $\triangle$ ) and expected charge values ( $\square$ ). C. Charge from MG motor compound action potentials ( $\nabla$ ) and expected charge values ( $\square$ ). Points are plotted as in Figure 12B. Regression parameters are listed in Table III.





#### IV. DISCUSSION

The results of the present series of experiments point out that while changes in conduction velocity distributions account for a large proportion of the loss of compound action potential charge following axotomy, there is a significant loss in the number of conducting fibers. Fast conducting efferent fibers degenerate less rapidly than either fast conducting muscle or cutaneous afferent fibers. In contrast, there is little difference between the rates of degeneration of slow conducting fibers in any of these three categories. Furthermore, although fast conducting afferent fibers of both types degenerate faster than slow conducting afferents, no difference is evident between alpha- and gamma-motoneurons.

The present findings not only confirm the findings of Hoffer et al. (1979) "that following axotomy large myelinated sensory fibers are substantially more affected than motor fibers in the same peripheral nerves," but also show that muscle and cutaneous afferent fibers are affected to more or less the same degree.

The observed declines in conduction velocity and compound action potential charge are to a large extent the products of nerve fiber atrophy. As the total fiber diameter decreases conduction velocity slows with a concomitant reduction in the amplitude and charge of a single unit potential. This is well-known from empirical data (Gasser & Grundfest, 1939) and is predicted on the basis of



theoretical considerations (Stein & Pearson, 1971, Moore et al., 1978). Fiber diameter distributions determined from histological sections, however, do not appear to be good measures of the conduction velocity distributions of degenerating nerves. Cumulative fiber diameter histograms derived from measurements of total fiber diameter showed a much less pronounced shift toward the smaller end of the spectrum than the corresponding shift toward slower conduction velocities in the conduction velocity distributions (Gillespie and Hanley, unpublished observations).

However, degenerating fibers no longer present a normal morphological picture. Myelin layers begin to separate and break up, swellings containing vacuolated macrophages or ovoids of myelin debris appear at irregular intervals along the axon and myelin bubbles appear near the neuroma (Spencer & Lieberman, 1971). Histological sections of axotomized nerves from this study often showed an almost complete disappearance of the axoplasmic interior of nerve fibers without a proportionate reduction in the thickness of the surrounding myelin-sheath, thereby dramatically reducing the ratio of axon to total fiber diameter. Atrophying axons were generally quite irregular in shape. Some of the axons which were allowed to degenerate for long periods were almost completely filled with osmiophilic material. Rather than functional axons, these may have been the debris-filled swellings identified by Spencer and Lieberman. It may be



questioned to what extent any of the abnormal axons were functional. In fact, several nerves which had few, if any, axons of normal appearance were still able to conduct action potentials albeit at conduction velocities much slower than control values. Prediction of conduction velocity distributions on the basis of fiber diameter histograms of axons of such abnormal appearance would have been extremely difficult and highly inaccurate.

Cragg and Thomas (1961) claimed that myelin-sheath thickness and axon diameter were reduced proportionately in atrophying nerve fibers. This is contrary to the present findings and to the findings of others as reviewed by Sunderland (1978). Nevertheless, even if it were true, Cragg and Thomas did not find a very good linear correlation between the changes in diameter and the changes in conduction velocity such as would be expected for normal nerves. Changes in conduction velocity of 20-50% corresponded to changes in diameter of only 10-20%. This prompted them to suggest "that the changes in axon diameter and myelin-sheath thickness may be accompanied by changes in their electrical properties." Such changes could certainly alter the conduction velocity significantly, according to the computer simulations of Moore et al. (1978). On the other hand, Stein and Pearson (1971) showed that action potential amplitude is much less dependent on changes in rate constants, conductance and capacity. A significant change in the relationship between single unit potential





amplitude and conduction velocity might therefore have been expected following axotomy. The data presented in Figures 5, 6 and 7 give little evidence of such a change since points from late experiments fit the computed lines as well as those from early experiments.

This also suggests that axonal sprouting did not distort conduction velocity distributions and charge values which were assumed to have been obtained from parent fibers only. Had potentials been recorded from the region of sprouting, there should have been much more scatter in the single unit potential data. For example, a single unit potential recorded from a small diameter, thinly myelinated sprout at the distal end of a fast conducting fiber should have had a much lower amplitude than normal for a single unit potential of that particular conduction velocity. Although the nerves were recut as far proximal to the neuroma as possible for recording, some groups of small, thinly myelinated axons, assumed to be sprouts, were seen in histological sections taken from the portion of the MG nerve from which single unit potentials were recorded. Perhaps, these were fibers which had turned in the neuroma and grown back up the central stump (Aitken, 1949). McQuarrie (1979) found that the maximum extent of 'traumatic degeneration' for the largest myelinated fibers extended only several millimeters proximal to the point of nerve section and that this was also proximal to the zone of sprout formation. This also suggests that any sprouts at the site of recording,





which was usually 15-20 mm proximal to the neuroma, had in fact grown in the retrograde direction. Since the nerve was ligated and cut proximal to the neuroma prior to recording, these fibers would not have contributed to the compound action potential and would not have been among the single unit potentials sampled. Few sprouts were seen in sections taken from the site of recording on the sural nerve. Because the sural was generally cut more than 20 mm from the neuroma, this was probably beyond the proximal extent of any sprouting.

The question of the extent of cell death, if any, following axotomy, which Hoffer et al. (1979) were unable to answer has still not been clearly resolved. Carlson et al. (1979) claimed that while nerve fibers in the L7 ventral root of amputated hindlimbs were reduced in diameter there was no significant loss in the number of axons or cell bodies after 18 months. In contrast, there was a significant loss of both dorsal root fibers and ganglion cells (approximately 20%) in addition to a reduction in fiber diameter. Although such a loss of dorsal root ganglion cells might account for some of the difference between charge computed from the sensory conduction velocity distribution and the actual recorded charge, it seems unlikely that it could explain the discrepancy completely since they saw the greatest loss among the smaller cell bodies. Furthermore, their findings lead one to expect that the charge recorded from efferent fibers should not decay significantly faster



than that computed from the conduction velocity distribution. Since they do not describe the appearance of any of the surviving fibers no assessment can be made of the capacity to conduct impulses.

Recently, Jessell et al. (1979) have shown that there is a 75-80% depletion of substance P from the dorsal horn following sciatic nerve section. They suggest that this probably reflects the degeneration of substance P containing neurons. This is consistent with Carlson's findings mentioned above, since so far substance P has been identified only in the small diameter myelinated afferents (Hökfelt et al., 1977). In addition, it indicates that the apparent loss of slow conducting fibers seen in the sural nerve soon after axotomy is in fact real.

Support for the differential degeneration of fast and slow conducting afferent fibers may be derived from differences in the rates of regeneration and maturation following nerve crush. Devor and Govrin-Lippmann (1979a) have shown that fast conducting fibers regenerate more quickly than slow conducting fibers and that recovery of conduction velocity in regenerating sprouts occurs at faster rates in fast conducting fibers than slow conducting fibers (1979b). The rate of regeneration of the axon sprout may reflect the rate of degeneration of the parent fiber if fibers which regenerate faster initially divert more of their metabolic energy to the growing sprout and consequently allow catabolism of constituents of the parent





axon.

Although the present study offers no way of distinguishing between the roles played by trophic factors such as nerve growth factor, for example, and ongoing electrical activity in maintaining the viability of nerve fibers, the fact that fast conducting afferents deteriorate at the fastest rate suggests that both the frequency and the total amount of impulse traffic along an axon following axotomy, relative to that normally generated, may be important in determining the rate of degeneration. Both afferents and efferents remain active following axotomy (Govrin-Lippmann & Devor, 1978, Stein et al., 1979) but the amount of sensory activity falls far more quickly than motor activity. Both alpha- and gamma-motoneurons can be excited centrally. Afferent fibers, on the other hand, are dependent on phenomena associated with regeneration for the production of impulses in the absence of normal end organs. Some afferent activity is generated in the region of the neuroma and additional activity may result from electrical interactions between sensory and motor fibers (Seltzer & Devor, 1979). The neural activity generated as a consequence may be sufficient to sustain slowly conducting afferents which are normally relatively silent but may not provide enough activity for fast conducting fibers which normally generate high frequency bursts of impulses.

Czéh et al. (1977) have shown that while disuse of muscle afferents does cause a small reduction in conduction





velocity, this slowing is substantially less than that observed following axotomy. Similar disuse of alpha-motoneurons (Czéh et al., 1978) leads only to changes in the electrical properties of the cell body without affecting axonal conduction velocity. These findings suggest that trophic factors play a primary role in preserving the functionality of an axon, although electrical activity may be significant in determining the differential effects on various classes of axons. The exact nature of the trophic role of electrical activity is not yet known and awaits further investigation.



## V. SUMMARY

1. Severance of peripheral nerves results in irreversible retrograde degeneration of axons when reinnervation is prevented.
2. The effects of axotomy differ for sensory and motor fibers as manifested by changes in compound action potential charge and conduction velocity distributions.
3. The rate of charge decay is significantly faster in sensory than motor fibers.
4. Analysis of changes in conduction velocity distributions following axotomy show that fast conducting sensory fibers are most severely affected, having the fastest initial rates of conduction velocity decay.
5. The conduction velocities of slow sensory and motor fibers and fast motor fibers appear to decay at more or less the same rates.
6. It is suggested that the amount of electrical activity in nerve fibers following axotomy relative to that present prior to axotomy may play a role in determining the rate at which electrophysiological degeneration proceeds.



## REFERENCES

- Aitken, J.T. (1949). The effect of peripheral connexions on the maturation of regenerating nerve fibers. *J. Anat.* 83, 32-43.
- Barker, A.T., Brown, B.H. and Freeston, I.L. (1979). Determination of the distribution of conduction velocities in human nerve trunks. *IEEE Trans. Biomed. Eng.* BME-26, 76-81.
- Blair, E.A. and Erlanger, J. (1933). A comparison of the characteristics of axons through their individual electrical pulses. *Amer. J. Physiol.* 106, 524-564.
- Boyd, I.A. and Kalu, K.U. (1979). Scaling factor relating conduction velocity and diameter for myelinated afferent nerve fibers in the cat hind limb. *J. Physiol.* 289, 277-297.
- Buchthal, F. and Rosenfalck, A. (1966). Evoked action potentials and conduction velocity in human sensory nerves. *Brain Research* 3, 1-122.
- Bucy, P.C. (1928). Studies in degeneration of peripheral nerves. *J. Comp. Neurol.* 45, 129-159.
- Carlson, J., Lais, A. and Dyck, P.J. (1979). Axonal atrophy from permanent peripheral axotomy in adult cats. *J. Neuropath. Exp. Neurol.* 38, 579-585.
- Cragg, B.G. and Thomas, P.K. (1961). Changes in conduction velocity and fiber size proximal to peripheral nerve lesions. *J. Physiol.* 157, 315-327.
- Cragg, B.G. and Thomas, P.K. (1964). The conduction velocity of regenerated peripheral nerve fibers. *J. Physiol.* 171, 164-175.
- Cummins, K.L., Perkel, D.H. and Dorfman, L.J. (1979). Nerve fiber conduction-velocity distributions. I. Estimation based on the single-fiber and compound action potentials. *EEG Clin. Neurophysiol.* 46, 634-646.
- Czéh, G., Kudo, N. and Kuno, M. (1977). Membrane properties and conduction velocity in sensory neurones following central or peripheral axotomy. *J. Physiol.* 270, 165-180.
- Czéh, G., Gallego, R., Kudo, N. and Kuno, M. (1978). Evidence for the maintenance of motoneurone properties by muscle activity. *J. Physiol.* 281, 239-252.





- Davis, L.A., Gordon, T., Hoffer, J.A., Jhamandas, J. and Stein, R.B. (1978). Compound action potentials recorded from mammalian peripheral nerves following ligation or resuturing. *J. Physiol.* 285, 543-559.
- Devor, M. and Govrin-Lippmann, R. (1979a). Maturation of axonal sprouts after nerve crush. *Exp. Neurol.* 64, 260-270.
- Devor, M. and Govrin-Lippmann, R. (1979b). Selective regeneration of sensory fibers following nerve crush injury. *Exp. Neurol.* 65, 243-254.
- Edwards, A.L. (1976). *An Introduction to Linear Regression and Correlation*. W.H. Freeman, San Francisco.
- Faddeev, D.K. and Faddeeva, V.N. (1963). *Computational Methods of Linear Algebra*. W.H. Freeman, New York.
- Fleming, R.A. (1896). Some notes on ascending degeneration (so-called) and on the changes in nerve cells consequent thereon. *Br. Med. J.* 2, 918-921.
- Gasser, H.S. and Erlanger, J. (1927). The role played by the sizes of the constituent fibers of the nerve trunk in determining the form of its action potential wave. *Amer. J. Physiol.* 80, 522-545.
- Gasser, H.S. and Grundfest, H. (1939). Axon diameters in relation to the spike dimensions and the conduction velocity in mammalian A fibers. *Amer. J. Physiol.* 127, 393-414.
- Govrin-Lippmann, R. and Devor, M. (1978). Ongoing activity in severed nerves: source and variation with time. *Brain Research* 159, 406-410.
- Gutmann, E. and Holubář, J. (1950). The degeneration of peripheral nerve fibers. *J. Neurol. Neurosurg. Psychiat.* 13, 89-105.
- Hoffer, J.A., Stein, R.B. and Gordon, T. (1979). Differential atrophy of sensory and motor fibers following section of cat peripheral nerves. *Brain Research* 178, 347-361.
- Hökfelt, T., Johansson, O., Kellerth, J.-O., Ljungdahl, A., Nilsson, G., Nygårds, A. and Pernow, B. (1977). Immunohistochemical distribution of substance P. In *Substance P*, eds. U.S. von Euler and B. Pernow, pp. 117-145. Raven Press, New York.



- Jessell, T., Tsunoo, A., Kanazawa, I. and Otsuka, M. (1979). Substance P: depletion in the dorsal horn of rat spinal cord after section of the peripheral processes of primary sensory neurons. *Brain Research* 168, 247-259.
- Kiraly, J.K. and Krnjević, K. (1959). Some retrograde changes in function of nerves after peripheral section. *Quart. J. Exp. Physiol.* 44, 244-257.
- Kovacs, Z.L., Johnson, T.L. and Sax, D. (1979). Estimation of the distribution of conduction velocity in peripheral nerves. *Comput. Biol. Med.* 9, 281-293.
- Landau, W.M., Clare, M.H. and Bishop, G.H. (1968). Reconstruction of myelinated nerve tract action potentials: an arithmetic method. *Exp. Neurol.* 22, 480-490.
- Lee, R.G., Ashby, P. White, D.G. and Aguayo, A.J. (1975). Analysis of motor conduction velocity in human median nerve by computer simulation of compound muscle action potentials. *EEG Clin. Neurophysiol.* 39, 225-237.
- Leifer, L., Meyer, M., Morf, M. and Pertig, B. (1977). Nerve bundle conduction velocity distribution measurement and transfer function analysis. *Proc. IEEE* 65, 747-755.
- McQuarrie, I.G. (1975). Accelerated axonal sprouting after nerve transection. *Brain Research* 167, 185-188.
- Moore, J.W., Joiner, R.W., Brill, M.H., Waxman, S.G. and Najaar-Joa, M. (1978). Simulations of conduction in uniform myelinated fibers. Relative sensitivity to changes in nodal and internodal parameters. *Biophys. J.* 21, 147-160.
- Olson, W.H. (1973). *Peripheral Nerve Compound Action Potentials and Fiber Diameter Histograms*. (Ph.D. dissertation) University of Michigan.
- Paintal, A.S. (1966). The influence of diameter of medullated nerve fibers of cats on the rising and falling phases of the spike and its recovery. *J. Physiol.* 184, 791-811.
- Seltzer, Z. and Devor, M. (1979). Ephaptic transmission in chronically damaged peripheral nerves. *Neurol.* 29, 1061-1064.
- Spencer, P.S. and Lieberman, A.R. (1971). Scanning electron microscopy of isolated peripheral nerve fibers: normal structure and alterations proximal to neuromas. *Z. Zellforsch.* 119, 534-551.





- Stein, R.B. and Pearson, K.G. (1971). Predicted amplitude and form of action potentials from unmyelinated nerve fibers. *J. Theor. Biol.* 32, 539-558.
- Stein, R.B. and Oğuztöreli, M.N. (1978). The radial decline of nerve impulses in a restricted cylindrical extracellular space. *Biol. Cybernetics* 28, 159-165.
- Stein, R.B., Hoffer, J.A., Gordon, T., Davis, L.A., and Charles, D. (1979). Long-term recordings from cat peripheral nerves during degeneration and regeneration: implications for human nerve repair and prosthetics. In *Nerve Repair: Its Clinical and Experimental Basis*, eds. D.L. Jewett and H.R. McCarrol, pp. 166-176. C.V. Mosby, St. Louis.
- Sunderland, S. (1978). *Nerve and Nerve Injuries*. Livingstone, Edinburgh.
- Williams, W. (1972). Transfer characteristics of dispersive nerve bundles. *IEEE Trans. Sys. Man Cybernetics* SMC-2, 72-85.
- Young, J.Z. (1942). The functional repair of nervous tissue. *Physiol. Rev.* 22, 318-374.





## APPENDIX I

## Computation of the Conduction Velocity Distribution

Given that the single unit potential (SUP) waveform varied with conduction velocity only and that SUPs sum linearly to produce the recorded compound action potential (CAP), the CAP may be expressed in the following form:

$$C(t) = \sum_{i=1}^N w_i f_i(t - d_i) \quad (1)$$

where  $C(t)$  = the recorded CAP as a function of time

$N$  = the number of fiber classes

$w_i$  = the amplitude-weighting coefficient for fibers in conduction velocity class  $i$

$f_i(t)$  = the SUP for the conduction velocity class  $i$

$d_i$  = the propagation delay for fibers in class  $i$

The  $f_i(t)$  are normalized with any amplitude dependence on conduction velocity incorporated into the weighting coefficients  $w_i$ . The major factors determining the delay times  $d_i$ , i.e., the time elapsed from the instant of nerve activation until the action potential arrives at the recording site, are the distance travelled along the nerve and the velocity of propagation, i.e.,

$$d_i = L/v_i \quad (2)$$

where  $L$  = measured distance from the stimulating cathode to the recording site

$v_i$  = the conduction velocity represented by class  $i$

'Virtual' cathode effects and activation times are neglected here because the delays which they introduce are small in comparison to the conduction time which was always



greater than 1 msec.

The weighting coefficients  $w_i$  are assumed to be of the form:

$$w_i = M_i k v_i^n \quad (3)$$

where  $M_i$  = the number of fibers activated in class  $i$

$k$  = an empirically determined constant

$n$  = an empirically determined exponent

The values of  $k$  and  $n$  were determined experimentally by plotting SUP amplitude against conduction velocity. The values are listed in Table I. The value of  $k$  is not needed to determine the normalized conduction velocity distribution since it can be factored from Eqn. (1) and therefore disappears upon normalization.

The CAP model of Eqn. (1) can be formulated in terms of discrete time by using equally spaced samples for the SUP and CAP functions. Eqn. (1) then becomes

$$C(t_k) = \sum_{i=1}^N w_i f_i(t_k - d_i) \quad (4)$$

where  $t_k$  is the  $k$ th time point.

Assuming that there are  $K$  values of the CAP, Eqn. (4) may be written in matrix form

$$c = Fw \quad (5)$$

where  $c$  = a  $K \times 1$  column vector of  $K$  time samples of the CAP

$F$  = a  $K \times N$  matrix whose  $i$ th column is the sampled SUP function  $f_i(t_k - d_i)$

$w$  = an  $N \times 1$  column vector of the  $N$  weighting coefficients

In estimating the conduction velocity distribution from



a recorded CAP and known SUP properties, Eqn. (5) may be viewed as a set of  $K$  equations in  $N$  unknowns (the  $w_i$ ). If the matrix  $F$  were square (i.e. if  $K = N$ ) and non-singular, the vector  $w$  could be determined. In general, it is not desirable to have  $K = N$ . Rather the number of time samples should exceed the number of velocity classes (Barker et al., 1979, Cummins et al., 1979). The system of simultaneous linear equations is then overdetermined. A least-squares fit can be found for the vector  $w$  by premultiplying both sides of Eqn. (5) by the transpose of the matrix  $F$

$$F^T C = F^T F w \quad (6)$$

and solving to obtain  $w$ .

If the columns of the matrix  $F$  are chosen to represent SUPs having different delay times then they will be independent and the system will have a unique solution. Because of the symmetry of  $F^T F$ , Eqn. (6) can be solved for  $w$  by using the square-root method (Fadeev and Fadeeva, 1963).

A FOCAL program was written to compute a conduction velocity distribution with 38 conduction velocity classes, chosen so as to have conduction latencies which differed by a least one sample period of the digitized CAP. The choice of 38 classes was somewhat arbitrary having been dictated to a large extent by the amount of computer memory available. SAPs representing individual conduction velocity classes were obtained by scaling the duration of the SUP template (see Methods) according to the experimentally determined relationship between half-width and conduction velocity. The





scaling was done by linear interpolation so as to preserve the SUP waveshape. Each conduction velocity class had an associated delay time  $d_i$  calculated from Eqn. (2). In this way the sampled SUP functions  $f_i(t_k - d_i)$  of Eqn. (4) were determined and subsequently used to construct the F matrix.

The program computed  $F^T F$  and using the CAP vector  $c$  found the least-squares estimate of the weighting vector  $w$  by the square-root method. The weighting coefficients  $w_i$  were then scaled by  $v_i^{-n}$  to calculate the values of  $M_i$  which constituted the conventional conduction velocity distribution. The  $M_i$  were then accumulated and normalized to generate the cumulative conduction velocity distribution.



## APPENDIX II

## Regression Analysis of Data

Data points were fitted with curves of the form  $y = Ae^{-Bt}$  or  $y = kv^n$  using the transformations  $\ln(y) = \ln(A) - Bt$  or  $\ln(y) = \ln(k) + n\ln(v)$  respectively. Correlation coefficients and standard errors were calculated according to standard equations for linear regression (see Edwards, 1976). Regression coefficients from different populations were tested for significant differences by testing the null hypothesis.

Decay curves of the form  $Ae^{-Bt} + C$  were obtained by computing parameters which minimized the residual sum of squares. A non-linear regression analysis program was employed. This program is available in the BMDP package of programs for biomedical applications developed at the Health Sciences Facility of the University of California, Los Angeles.

Note that all data points were used in calculating parameters although in some cases only the means of grouped points were plotted in order to prevent graphs from becoming too cluttered.







**B30285**